

CATALYST SCREENING AND TESTING FOR STEAM REFORMING OF  
METHANE TO SYNTHESIS GAS

by

Nilay Aktürk

B.S., Chemical Engineering, Yıldız Technical University, 2008

Submitted to the Institute for Graduate Studies in  
Science and Engineering in partial fulfillment of  
the requirements for the degree of

Master of Science

Graduate Program in Chemical Engineering

Boğaziçi University

2011

*to my family*

## ACKNOWLEDGEMENTS

First of all, I would like to express my truthful gratitude to my thesis supervisor Assoc. Prof. Ahmet Kerim Avcı, who devoted his valuable time to guiding me, helping me and motivating me all the time. It was a great honor for me to work with him during my graduate thesis, where I learned from his great expertise and experiences in catalysis and reaction engineering. I also thank to Prof. Zeynep İlsen Önsan and Prof. Ayşe Nilgün Akın, who have read and commented on my thesis.

Special thanks are due to A. İpek Paksoy, Melek Selcen Başar, Mustafa Karakaya, Eyüp Şimşek for their enjoyable friendship and sharing their experiences with me. I would like to thank my friends that I have met during my M. S. study making this two year cheerful and enjoyable. Many thanks to İhsan Ömür Akdağ, Vasfiye Çimenoğlu, Pınar Derin, Aslıgül Doğan, Murat Erol, Merve Eropak, Gülsüm Ersoy, Mehmet Ünal Güneş, Mehmet İrfan Hösükoğlu, Duygu Kocaman, Aybüke Leba, Çağlar Meriçer, Bahar Nalbantoğlu, Şefik Kerem Ovalı, Ali Uzun, Caner Ülgüel, Simay Yalaz, Okan Yüzüak.

I would like to thank Nicolas Chateau, Aidin Dario, Ebru Doğan, Erdem Eren, Selçuk Hazar, Özer Özcan, Arman Savran, Hasan Özgen Sicim, Gülgün Ural and Osman Yüksel for their friendship. Burcu Selen Çağlayan, Feyza Gökalliler and Tuğba Davran Candan deserve special thanks as mentors of the CATREL team. Their invaluable experience and will to help has made this study possible. Cordial thanks for Bilgi Dedeoğlu and Nurettin Bektaş for their technical assistance and significant efforts during my thesis and also Yakup Bal for his friendly attitude.

Finally, I would like to thank my family for their unrequited support and trust in me throughout my thesis like my whole life. This work is dedicated to them, without whom it would have never been possible.

Financial support for this study is provided by TÜBİTAK through project MAG-108M509 and by TÜBA-GEBİP program.

## ABSTRACT

### CATALYST SCREENING AND TESTING FOR STEAM REFORMING OF METHANE TO SYNTHESIS GAS

The major aim of this study is to investigate the effects of different metals and supports on methane conversion and carbon monoxide selectivity in steam reforming (SR) of methane. The test matrix involves the investigation of 15wt% Ni/ $\delta$ -Al<sub>2</sub>O<sub>3</sub>, 1wt% Pd/ $\delta$ -Al<sub>2</sub>O<sub>3</sub>, 2wt% Pt/ $\delta$ -Al<sub>2</sub>O<sub>3</sub>, 2wt% Rh/ $\delta$ -Al<sub>2</sub>O<sub>3</sub>, 2wt% Ru/ $\delta$ -Al<sub>2</sub>O<sub>3</sub>, 15wt% Ni/TiO<sub>2</sub>, 1wt% Pd/TiO<sub>2</sub>, 2wt% Pt/TiO<sub>2</sub>, 2wt% Rh/TiO<sub>2</sub>, 2wt% Ru/TiO<sub>2</sub>, 15wt% Ni/CeO<sub>2</sub>, 1wt% Pd/CeO<sub>2</sub>, 2wt% Pt/CeO<sub>2</sub>, 2wt% Rh/TiO<sub>2</sub>, 2wt% Ru/TiO<sub>2</sub> catalysts, all of which are in particulate form. The catalysts are prepared by the incipient-to-wetness impregnation method and catalytic activity tests were carried out in a continuous flow micro-reactor system. During the experiments, reaction temperature and molar steam-to-carbon ratio at the inlet are kept constant at 700 °C and at 2.5, respectively.

The catalysts performances are investigated in terms of CH<sub>4</sub> conversion and CO selectivity results. It has been observed that CeO<sub>2</sub> supported Ni catalyst exhibited the better performance in terms of methane conversion and carbon monoxide selectivity than  $\delta$ -Al<sub>2</sub>O<sub>3</sub> and TiO<sub>2</sub>. For precious metals (Pd, Pt, Rh, Ru), however, CeO<sub>2</sub> exhibited lower CO selectivity than  $\delta$ -Al<sub>2</sub>O<sub>3</sub> and TiO<sub>2</sub>, both of which gave similar selectivities. For all supports, Rh was found to be the most active metal. The catalytic activities are found to follow the decreasing order of Rh = Ni > Pt > Pd > Ru for  $\delta$ -Al<sub>2</sub>O<sub>3</sub>, Rh = Ni > Ru > Pt > Pd for CeO<sub>2</sub> and Rh > Ru > Pd > Ni > Pt for TiO<sub>2</sub>. TiO<sub>2</sub> supported catalysts showed more stable behavior than the  $\delta$ -Al<sub>2</sub>O<sub>3</sub> and CeO<sub>2</sub> supported ones.

## ÖZET

### BUHAR REFORMLAMASI İLE METANDAN SENTETİK GAZ ÜRETİMİ İÇİN KATALİZÖR HAZIRLANMASI VE DENENMESİ

Bu çalışmanın ana amacı, metan buhar reformlanmasında farklı metallerin ve destek malzemelerinin, metan dönüşümü ve CO seçiciliği üzerindeki etkilerinin araştırılmasıdır. Deney planı, tanecikli yapıya sahip, (ağırlıkça) %15 Ni/ $\delta$ -Al<sub>2</sub>O<sub>3</sub>, %1 Pd/ $\delta$ -Al<sub>2</sub>O<sub>3</sub>, %2 Pt/ $\delta$ -Al<sub>2</sub>O<sub>3</sub>, %2 Rh/ $\delta$ -Al<sub>2</sub>O<sub>3</sub>, %2 Ru/ $\delta$ -Al<sub>2</sub>O<sub>3</sub>, %15 Ni/TiO<sub>2</sub>, %1 Pd/TiO<sub>2</sub>, %2 Pt/TiO<sub>2</sub>, %2 Rh/TiO<sub>2</sub>, %2 Ru/TiO<sub>2</sub>, %15 Ni/CeO<sub>2</sub>, %1 Pd/CeO<sub>2</sub>, %2 Pt/CeO<sub>2</sub>, %2 Rh/TiO<sub>2</sub> ve %2 Ru/TiO<sub>2</sub> katalizörlerinin incelenmesini kapsamaktadır. Katalizörler, emdirme yöntemiyle hazırlanmış ve aktivite deneyleri, sürekli akışlı mikro-reaktör deney sisteminde yapılmıştır. Tüm deneylerde, reaksiyon sıcaklığı ve molar buhar karbon oranı, sırasıyla 700 °C ve 2.5'te sabit tutulmuştur.

Katalizör performansları, CH<sub>4</sub> dönüşümü ve CO seçiciliği sonuçlarına göre incelenmiştir. CeO<sub>2</sub> destekli Ni katalizörü, CH<sub>4</sub> dönüşümü ve CO seçiciliği açısından,  $\delta$ -Al<sub>2</sub>O<sub>3</sub> ve TiO<sub>2</sub>'ya göre daha iyi performans göstermiştir. Fakat, değerli metaller (Pd, Pt, Rh, Ru) için, CeO<sub>2</sub>, benzer seçicilik davranışları gösteren  $\delta$ -Al<sub>2</sub>O<sub>3</sub> ve TiO<sub>2</sub>'ya göre düşük CO seçiciliği vermiştir. Bütün katalizör destekleri için, Rh en aktif metal olarak tespit edilmiştir. Katalitik aktiviteler,  $\delta$ -Al<sub>2</sub>O<sub>3</sub> için Rh = Ni > Pt > Pd > Ru, CeO<sub>2</sub> için Rh = Ni > Ru > Pt > Pd, TiO<sub>2</sub> için Rh > Ru > Pd > Ni > Pt sırasını takiben azalmıştır. TiO<sub>2</sub> destekli katalizörler,  $\delta$ -Al<sub>2</sub>O<sub>3</sub> ve CeO<sub>2</sub> desteklilerine göre genellikle daha kararlı davranış göstermişlerdir.

## TABLE OF CONTENTS

ACKNOWLEDGEMENT .....	iv
ABSTRACT .....	v
ÖZET .....	vi
LIST OF FIGURES .....	ix
LIST OF TABLES .....	xi
LIST OF SYMBOLS/ABBREVIATIONS .....	xii
1. INTRODUCTION .....	1
2. LITERATURE SURVEY .....	3
2.1. Synthesis gas .....	3
2.2. Steam Reforming of Methane .....	4
2.3. Catalysts for Steam Reforming of Methane .....	7
2.3.1. Particulate Catalysts.....	7
2.3.2. Monolithic Catalysts .....	8
2.4. Catalyst Supports .....	10
3. EXPERIMENTAL WORK .....	13
3.1. Materials .....	13
3.1.1. Chemicals .....	13
3.1.2. Gases and Liquids .....	14
3.2. Experimental System .....	14
3.2.1. Catalyst Preparation Systems .....	15
3.2.2. Catalytic Reaction System .....	16
3.2.3. Catalytic Product Analysis System.....	16
3.3. Catalyst Preparation and Pretreatment .....	18
3.3.1. Support Preparation.....	18
3.3.1.1. Alumina .....	18
3.3.1.2. Titania.....	18
3.3.1.3. Ceria.....	18
3.3.1.4. Preparation of Ni/ $\delta$ -Al <sub>2</sub> O <sub>3</sub> Catalyst .....	20
3.3.1.5. Pretreatment of Catalysts .....	20
3.4. Reaction Tests .....	22

3.4.1. Preliminary Work.....	22
3.4.2. Blank Tests .....	22
3.4.3. Steam Reforming of Methane over Studied Catalysts.....	23
3.5. Design and Construction of the System .....	23
3.5.1. Feed Section .....	24
3.5.2. Reaction Section .....	25
3.5.3. Feed/Product Analysis Section .....	26
3.6. Methane Steam Reforming Experiments.....	30
3.6.1. Parameters of Activity.....	30
4. RESULTS AND DISCUSSION .....	32
4.1. Stability Comparison of Support Performance.....	32
4.2. CO Selectivity Comparison of Support Performance.....	38
5. CONCLUSIONS AND RECOMMENDATIONS.....	44
5.1. Conclusions.....	44
5.2. Recommendations.....	45
APPENDIX A: CALIBRATION CURVES OF THE GAS CHROMATOGRAPH....	46
APPENDIX B: CALIBRATION CURVES OF THE MASS FLOW CONTROLLERS.....	49
REFERENCES .....	52

## LIST OF FIGURES

Figure 3.1.	The impregnation system .....	15
Figure 3.2.	The HDP system .....	16
Figure 3.3.	XRD Analysis of Ceria Sample-1.....	19
Figure 3.4.	XRD Analysis of Ceria Sample-2.....	19
Figure 3.5.	Schematic diagram of the reactor and furnace system .....	26
Figure 3.6.	Flow routing arrangement for data analysis in GC-1.....	27
Figure 3.7.	Flow routing arrangement for data analysis in GC-2.....	28
Figure 3.8.	The integrated microreactor flow and product analysis system .....	29
Figure 4.1.	Stability Comparison of Ni-metal on Different Supports .....	33
Figure 4.2.	Stability Comparison of Pd-metal on Different Supports .....	33
Figure 4.3.	Stability Comparison of Pt-metal on Different Supports.....	34
Figure 4.4.	Stability Comparison of Ru-metal on Different Supports.....	35
Figure 4.5.	Stability Comparison of Rh-metal on Different Support.....	35
Figure 4.6.	CO Selectivity of Ni-metal on Different Supports for 6 hr.....	38
Figure 4.7.	CO Selectivity of Pd-metal on Different Supports for 6 hr.....	39

Figure 4.8.	CO Selectivity of Pt-metal on Different Supports for 6 hr .....	40
Figure 4.9.	CO Selectivity of Ru-metal on Different Supports for 6 hr .....	41
Figure 4.10.	CO Selectivity of Rh-metal on Different Supports for 6 hr .....	41

## LIST OF TABLES

Table 3.1.	Chemicals used for catalyst preparation.....	13
Table 3.2.	Applications and specifications of the liquids used .....	14
Table 3.3.	Applications and specifications of the gases used .....	14
Table 3.4.	Reactant and product gas analysis conditions .....	17
Table 3.5.	The Prepared Catalysts .....	21
Table 3.6.	The Prepared Catalysts cont. ....	22
Table 3.7.	Specifications of the mass flow controllers .....	25
Table 4.1.	Activity Performance of TiO <sub>2</sub> Supported Catalysts.....	37
Table 4.2.	Activity Performance of $\delta$ -Al <sub>2</sub> O <sub>3</sub> Supported Catalysts.....	37
Table 4.3.	Activity Performance of CeO <sub>2</sub> Supported Catalysts.....	37
Table 4.4.	CO Selectivity % of TiO <sub>2</sub> -Supported Catalysts at 360 min.....	42
Table 4.5.	CO Selectivity % of $\delta$ -Al <sub>2</sub> O <sub>3</sub> -Supported Catalysts at 360 min.....	42
Table 4.6.	CO Selectivity % of CeO <sub>2</sub> -Supported Catalysts at 360 min.....	43

## LIST OF ABBREVIATIONS

ATR	Autothermal Reforming
GC	Gas Chromatograph
FC	Fuel Cell
HPLC	High Performance Liquid Chromatography
ID	Inside Diameter
IPOX	Indirect Partial Oxidation
PEMFC	Proton Exchange Membrane Fuel Cell
LPG	Liquid Petroleum Gas
OSR	Oxidative Steam Reforming
PO	Partial Oxidation
POX	Partial Oxidation
PROX	Preferential Oxidation
S/C	Molar steam-to-carbon ratio at the inlet
SRM	Steam Reforming of Methane
SR	Steam Reforming
T	Temperature
TCD	Thermal Conductivity Detector
TOX	Total Oxidation
TPR	Temperature programmed reduction
WGS	Water-Gas Shift Reaction

## 1. INTRODUCTION

Renewed attention in both academic and industrial research has recently been focused on alternative routes for conversion of natural gas (methane) to synthesis gas, a mixture of CO and H<sub>2</sub>, which can be used to produce chemical products, such as hydrocarbons and oxygenated compounds. In GTL (gas-to-liquid) plants, where natural gas is first converted to synthesis gas, which is the feedstock for Fischer-Tropsch synthesis of hydrocarbons, where, above 60% -70% of the cost of the overall process is associated with the production of synthesis gas (Souza *et al.*, 2006; Rostrup-Nielsen, 1994). Therefore, reduction in synthesis gas generation costs would have a large and direct influence on the overall economics of these downstream industrial processes. Steam reforming of methane (SRM) is the most important industrial process for production of synthesis gas. SRM is highly endothermic and the H<sub>2</sub>/CO ratio obtained (> 3) is only suitable for processes requiring a H<sub>2</sub>-rich feed (such as ammonia synthesis and petroleum refining process, fuel cells), but it is too high for fuel synthesis *via* Fischer-Tropsch reaction (Souza *et al.*, 2006; Pena *et al.*, 2006, 1996; Tsang *et al.*, 1995). Catalytic partial oxidation (POX) of hydrocarbons is mildly exothermic and the H<sub>2</sub>/CO ratios in the product gas are more appropriate for Fischer-Tropsch synthesis but not for clean hydrogen generation. In more recently proposed systems suitable for PEM fuel cell grade H<sub>2</sub> production, such as oxidative steam reforming (OSR) and auto-thermal reforming (ATR), the heat required for endothermic methane steam reforming is balanced by the exothermic total oxidation (TOX) of methane with the oxygen injected at the reformer inlet (Trimm and Önsan, 2001; Önsan, 2007).

Fuel cells have been shown remarkable progress as being future transportation fuel and for stationary and mobile small scale power applications due to a number of advantages (Ahmed and Krumpelt, 2001). Fuel cells offer a promising path for hydrogen based energy systems as clean, flexible, and efficient devices utilized in either stationary or portable power generation applications and in transportation (Barreto *et al.*, 2003; Lee *et al.*, 2005). A typical feed gas mixture to a fuel cell can be obtained by converting hydrocarbon fuels first into synthesis gas (syngas) in a reformer, and the ratio of H<sub>2</sub> to CO content varies with the type of hydrocarbon fuel (Öztürk, 2009). Steam reforming, which is

the most important industrial process for production of hydrogen, provides a high H<sub>2</sub>/CO ratio (> 3) suitable for fuel cell applications (Yan *et. al*, 2003).

The major aim of this study is to investigate the effects of different metals and supports on methane conversion and carbon monoxide selectivity in steam reforming (SR) of methane. For this purpose, the catalyst testing system is re-constructed to enable analysis at high temperatures. After this step, the catalysts are prepared by using five different metals on three different support materials to give 15wt% Ni/ $\delta$ -Al<sub>2</sub>O<sub>3</sub>, 1wt% Pd/ $\delta$ -Al<sub>2</sub>O<sub>3</sub>, 2wt% Pt/ $\delta$ -Al<sub>2</sub>O<sub>3</sub>, 2wt% Rh/ $\delta$ -Al<sub>2</sub>O<sub>3</sub>, 2wt% Ru/ $\delta$ -Al<sub>2</sub>O<sub>3</sub>, 15wt% Ni/TiO<sub>2</sub>, 1wt% Pd/TiO<sub>2</sub>, 2wt% Pt/TiO<sub>2</sub>, 2wt% Rh/TiO<sub>2</sub>, 2wt% Ru/TiO<sub>2</sub>, 15wt% Ni/CeO<sub>2</sub>, 1wt% Pd/CeO<sub>2</sub>, 2wt% Pt/CeO<sub>2</sub>, 2wt% Rh/TiO<sub>2</sub>, 2wt% Ru/TiO<sub>2</sub>. The catalysts are prepared by using the incipient-to-wetness impregnation method, and catalytic activity tests are carried out in the quartz micro-reactor system operated at a temperature of 700°C. All of the experiments are performed at a molar steam-to-carbon ratio of 2.5. Conversion of methane, H<sub>2</sub>/CO ratio and the CO selectivity are calculated and compared for each catalyst.

Chapter 2 includes a brief literature survey on syngas, catalysts and supports that were used in the literature for syngas production in addition to methane conversion technologies. Chapter 3 describes the experimental systems and the procedures used for catalyst preparation and catalytic activity measurement. Details of the bench-scale methane reformer/reactor and gas analysis system constructed and the experimental results obtained from the parametric studies conducted on methane SR is presented and discussed in Chapter 4. The main conclusions that can be drawn from this study and the recommendations for future studies are given in Chapter 5.

## 2. LITERATURE SURVEY

### 2.1. Sythesis Gas

Crude oil (petroleum) is known as the most important hydrocarbon-based fuel that is used to meet a vast variety of energy needs. However, because of the economic, environmental and availability concerns about the crude oil, use of alternative fuels such as natural gas is becoming more important. One of the significant uses of natural gas is related to its conversion to synthesis gas, in which methane – the main constituent of natural gas – is catalytically converted to synthesis gas (syngas), a mixture of CO and H<sub>2</sub>. Syngas is a notable mixture as it can be converted to liquid fuels via Fischer-Tropsch synthesis, to hydrogen, and to other chemicals (Chen *et. al*, 2003).

Syngas that can be used to produce methanol and synthetic fuels and hydrogen that can be used both in the chemical industry and for the generation of electrical energy via fuel cells are produced by highly endothermic steam reforming (SR) of natural gas. However, SR process provides a high H<sub>2</sub>/CO (>3) ratio which is not suitable for Fischer-Tropsch and methanol syntheses. Because of the desire of obtaining a more suitable H<sub>2</sub>/CO ratio for synthetic fuel production (~2), researches have been directed to methane partial oxidation (POX) or to CH<sub>4</sub>/CO<sub>2</sub> reforming (Yan *et. al*, 2003).

Partial oxidation of methane (POM) to syngas has advantages of the potential for fast, efficient and economical production of syngas. But the POM process has a disadvantage that cannot be easily controlled due to the diffucilty of removing the reaction heat from the reactor (Liu *et. al*, 2000; Yan *et. al*, 2003). Therefore, interests have been attracted on methane conversion to syngas via CO<sub>2</sub> reforming. Reforming methane with carbon dioxide is attractive for two reasons: (1) low H<sub>2</sub>/CO ratio ( $\leq 1$ ) is produced, which is suitable for Fischer-Tropsch synthesis of higher hydrocarbons, and (2) CO<sub>2</sub>, a greenhouse gas, is consumed in a useful manner. CH<sub>4</sub>/CO<sub>2</sub> reforming is strongly endothermic, and, therefore, high temperatures (800–1000°C) are required. These extreme temperatures are reported to promote carbon deposition, deactivate the catalyst, and sinter the supported metals (Matsukata *et al.*, 1996; Yan *et. al*, 2003).

Hydrogen is the ideal source of chemical energy that can be converted to electricity directly and efficiently via fuel cells with zero emissions of hazardous species (Avcı *et al.*, 2004). Due to the increase in H<sub>2</sub> demand and the importance of synthesis gas as a major feedstock for C<sub>1</sub> chemistry and fuel cells, methane reforming reactions have become more important. Notably, the on-site hydrogen production has received considerable attention because hydrogen could be utilized as an energy source for a proton exchange membrane fuel cell (PEMFC) for household use (Kusakabe *et al.*, 2004). However, hydrogen does not exist in pure form and is always combined with other elements such as oxygen and carbon. Therefore, it can be produced from all known energy systems based on different conventional primary energy carriers and sources besides being a by-product of many industrial processes (Gupta, 2009; Hordeski, 2009). The steam reforming of methane (SRM) is currently the most cost effective and highly developed method for production of hydrogen at relatively low cost and high H<sub>2</sub>/CO ratios as desired for hydrogen production (Profeti *et al.*, 2008; Salhi *et al.*, 2010).

## 2.2. Steam Reforming of Methane

There are three primary techniques that are used to produce hydrogen from hydrocarbon fuels: steam reforming, partial oxidation (POX), and autothermal reforming (ATR). Steam reforming of hydrocarbons is the most well-established process for commercial hydrogen production, and involves conversion of hydrocarbons into hydrogen and carbon oxides in the presence of steam over Ni-based catalysts. In this process oxygen is not needed and operating temperatures are generally lower than POX and ATR. The key reactions of methane steam reforming are illustrated below:



Steam reforming is an endothermic process, but the water-gas shift (2.3), which is slightly exothermic, accompanies the reforming reactions and affects the product distribution. The notable endothermicity of the reactions requires continuous supply of

external energy, and, based on this fact, degree of heat transfer to the process has a direct impact on hydrocarbon conversion and product selectivity (Steynberg and Dry, 2004). As a result, steam reforming reactors are designed to ensure efficient distribution of external heat to the catalyst particles.

In partial oxidation, hydrocarbons are converted to synthesis gas by their reaction with sub-stoichiometric amount of oxygen. Energy needed for the process is supported by the controlled combustion; once the reaction is triggered, the process becomes self-sustaining. A catalyst is not required for this process, but catalysts can be added to the system to decrease the operating temperatures. It may be difficult to control the temperature because of coke formation by reason of exothermic nature of the reactions. As the process can operate without a catalyst, the desulfurization requirements are less stringent compared to steam and autothermal reforming. However, partial oxidation has some drawbacks such as presence of very high operating temperatures ( $> \sim 1500$  °C), soot formation and production of low  $H_2/CO$  ratios that do not meet the feed specifications of Fischer-Tropsch synthesis (Holladay *et al.*, 2009).

Autothermal reforming, which is also known as oxidative reforming, is the combination of partial oxidation and the steam reforming. In this process, energy needed for steam reforming is supplied by partial oxidation, and the need for external energy demand is much less than needed in steam reforming. Compared to partial oxidation, autothermal reforming can run at lower process temperatures. Although it does not require an external heat source, it requires an expensive and complex oxygen separation unit to feed pure oxygen to the reactor. A summary of the main reactions of the three processes are given below (Holladay *et al.*, 2009):

Steam reforming:

$$C_mH_n + m H_2O = mCO + (m+(1/2)n)H_2; \Delta H = \text{hydrocarbon dependent, endothermic}$$

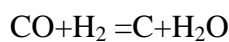
Partial Oxidation:

$$C_mH_n + 1/2mO_2 = mCO + 1/2nH_2; \Delta H = \text{hydrocarbon dependent, exothermic}$$

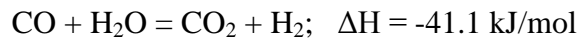
Autothermal reforming:

$C_mH_n + 1/2mH_2O + 1/4mO_2 = mCO + ((1/2)m + (1/2)n)H_2$ ;  $\Delta H =$  hydrocarbon dependent, thermally neutral

Carbon (coke) formation:



Water-gas shift:



Hydrocarbon steam reforming is highly endothermic and needs high reaction temperatures in excess of 600 K for oxygenated and 1000 K for saturated hydrocarbons. Such high temperatures may lead to catalyst deactivation by coke formation. To minimize the coking problem, the choice of catalyst and the water amount in the feed are very important (Önsan, 2007). The best steam to carbon ratio to avoid coking is greater than 2.5 for methane (Sperle *et al.*, 2005; Rostrup-Nielsen, 1998). Studies over different catalysts show that the addition of potassium, magnesia, alumina or molybdenum to supported Ni catalyst can also minimize the effects of carbon deposition during steam reforming of hydrocarbons (Borowiecki *et al.*, 2004; Borowiecki *et al.*, 1997).

In steam reforming process, direct conversion of methane produce a mixture of hydrogen, carbon monoxide and carbon dioxide in the presence of steam (Trimm and Önsan, 2001). Most strongly temperature plays a role on the amount of products and less strongly pressure. The higher the temperature is, the greater the amount of CO in the product. The CO amount will increase because of the effect of the temperature dependence of steam reforming and CO will be converted from produced CO<sub>2</sub> by rapid reverse WGS reaction (Semelsberger *et al.*, 2004). In steam reforming the reactions are typically endothermic, the energy needed for steam reforming is supplied from the heat generated by total oxidation of methane. As an advantage, the steam reforming process yields the

highest hydrogen concentration in the product among partial oxidation or autothermal reforming (Ahmed and Krumpelt, 2001; Brown, 2001).



In commercial applications of methane steam reforming Ni based catalysts are widely used because of their low price. However, precious metal catalysts like Rh or Ru are known to be more active than Ni, and also they promote less coke formation. The activities of various catalysts were reported as follows (Trimm and Önsan, 2001):



In industrial scale, steam reforming (SR) on Ni-based catalysts in packed bed tubular reactors is the most well known way for producing hydrogen from light hydrocarbons (Rostrup-Nielsen, 1984). However, this technology requires high energy inputs and large reactor volumes due to the slow kinetics and high endothermal heat of steam reforming (Avcı *et al.*, 2008). Steam reforming can operate at high temperatures up to 1100 K, and this brings the sintering problem of the catalyst. To prevent catalyst this problem, careful control of the bed temperature is required. In addition, coke formation can occur under SR conditions, but it can be eliminated when steam:carbon ratio is kept around 2.5 (Avcı *et al.*, 2002).

## 2.3. Catalysts for Steam Reforming of Methane

### 2.3.1. Particulate Catalysts

Rhodium is one of the most active and stable group VIII metals (Ni, Ru, Rh, Pt, Pd, Ir) which can catalyze the CH<sub>4</sub> reforming with steam or CO<sub>2</sub>. Studies have been investigating the activity of Rh based catalysts for steam reforming of methane over different supports. The catalytic steam reforming of methane is investigated over

Rh/Ce<sub>0.6</sub>Zr<sub>0.4</sub>O<sub>2</sub> catalyst by Halabi and his team over a temperature range of 475-725 °C. At low temperature most of the gas product is composed of CO<sub>2</sub> and H<sub>2</sub> because of the influence of water gas- shift reaction. At higher temperature and low steam to carbon ratio (S/C), this influence is diminished. Also, a molecular reaction mechanism is proposed to explain the kinetic observations. It is thought that two distinct sites are responsible for the dissociative adsorption of methane and steam on the catalyst and the support surfaces. Surface reactions of carbon containing methane precursors on the interface between the active metal and the support are considered to be the rate determining (Halabi *et al.*, 2010).

In one of the recent studies, a supported Fe<sub>2</sub>O<sub>3</sub>-Rh<sub>2</sub>O<sub>3</sub>/Y<sub>2</sub>O<sub>3</sub> catalyst was tested for partial oxidation of CH<sub>4</sub> to produce a synthesis gas (hydrogen and carbon monoxide) at 600-800 °C and it has showed promising outcomes (Nakayama *et al.*, 2008). Experiments have also been conducted for testing different support materials such as MgO, Al<sub>2</sub>O<sub>3</sub>, TiO<sub>2</sub>, Y<sub>2</sub>O<sub>3</sub>, La<sub>2</sub>O<sub>3</sub> and CeO<sub>2</sub> and Y<sub>2</sub>O<sub>3</sub> was found to be good choice for the support material.

In the study of Dagle and his coworkers (2008), Pd/ZnO/Al<sub>2</sub>O<sub>3</sub> catalyst was studied for water-gas-shift (WGS), methanol steam reforming, and reverse water-gas-shift (RWGS) reactions. The catalyst exhibited excellent WGS activity and stability, and found to be comparable to commercial Pt-based catalyst. Although Pd/ZnO/Al<sub>2</sub>O<sub>3</sub> is an active WGS catalyst, WGS is not involved in methanol steam reforming. RWGS rate constants are in the order of about 20 times lower than that of methanol steam reforming, proposing that RWGS reaction can be one of the sources for small amount of CO formation in methanol steam reforming (Dagle *et al.*, 2008).

In the study of Yan and his coworkers, Ni/TiO<sub>2</sub> catalyst was tested in partial oxidation of methane (POM) to syngas and in the CH<sub>4</sub>/CO<sub>2</sub> reforming reaction. It was found that Ni/TiO<sub>2</sub> catalyst provided long term stable catalytic activity during CO<sub>2</sub> reforming, while serious deactivation was observed during the POM process. TPR results demonstrated that nickel is mainly present as NiO and NiTiO<sub>3</sub> after the POM reaction. NiTiO<sub>3</sub> and NiO are not active as POM catalysts. Therefore, their formation has led to catalyst deactivation. No substantial buildup of surface carbonaceous species occurred and surface carbon was not the cause of the loss of catalyst activity in POM. Strong Ni/TiO<sub>x</sub> interaction and the presence of active oxygen within TiO<sub>2</sub> depressed the deposition of

carbon over Ni/TiO<sub>2</sub> catalyst. Thus, this catalyst showed stable activity during CH<sub>4</sub>/CO<sub>2</sub> reforming (Yan *et al.*, 2003).

In one of the recent studies, the effect of noble metal addition on the catalytic properties of Co/Al<sub>2</sub>O<sub>3</sub> was evaluated for the steam reforming of methane. Co/Al<sub>2</sub>O<sub>3</sub> catalysts were prepared with addition of different noble metals (Pt, Pd, Ru and Ir 0.3 wt.%) by a wetness impregnation method. Temperature programmed oxidation (TPO) analyses showed that the addition of the noble metals on the Co/Al<sub>2</sub>O<sub>3</sub> catalyst led to a more stable metallic state and less susceptible to the deactivation process during the reforming reaction. The Co/Al<sub>2</sub>O<sub>3</sub> promoted with Pt showed higher stability and selectivity for H<sub>2</sub> production during the methane steam reforming (Profeti *et al.*, 2008).

### 2.3.2. Monolithic Catalysts

Monolithic supports are structures that composed of interconnected repeating cells or channels. Monolithic supports are most commonly composed of ceramic or metal materials but some can also be made by plastic. The most important physical characteristic, when used as a catalyst support, is the size of the channel through which the gaseous reactants and products traverse (Heck *et al.*, 2001). The active catalyst is deposited as a washcoat onto the geometric surface of the monolithic structure. The washcoat is a mixture of active catalyst components, stabilizers, and a high surface area coating layer based on alumina (Giroux *et al.*, 2005). Reactors involving monolithic catalysts have several advantages compared with conventional fixed-bed reactors loaded with catalyst pellets, such as lower pressure drops, a smaller size and lower temperature gradients (Wu, *et.al.*, 2009)

The number of channels, their diameters and wall thickness determine the cell density, expressed as cells per square inch (cpsi), which in turn allows the calculation of the geometric surface area, the sum of the areas of all the channel walls upon which the catalyst is deposited. This leads to one of the most important advantages of the monolith in that it has a large open frontal area resulting in very little resistance to flow and hence low pressure drop. The lower the pressure drop the lower the resistance to flow or back pressure on the system and hence lower the energy loss (Heck *et al.*, 2001).

Although, the advantages of the monolith are many there are some disadvantages that prevent extensive use outside the environmental applications. The parallel channel monolith is essentially an adiabatic reactor limiting the control of temperature. In industry, for many exothermic or endothermic chemical and petroleum reactions selectivity is governed by the temperature so these types of monoliths are not suitable. Maybe that problem can be solved by a metal heat exchanger or metallic foam to control temperature but the amount of catalyst on the walls in a given volume of monolith is much less than a comparable volume of small diameter beads or extrudes. For chemical controlled reactions the monolith may not contain sufficient catalyst to yield the desired conversion efficiencies (Heck *et al.*, 2001).

#### 2.4. Catalyst Supports

Wang and Gorte (2002) carried out hydrocarbons steam reforming on three different catalysts, Pd/ceria, Pt/ceria and Pd/alumina. This study compared three catalysts and exhibited ceria- support excellent properties. It was found that, when compared to Pd/alumina, Pd/ceria gave higher rates and selectivities in steam reforming of hydrocarbons. The product selectivity (CO<sub>2</sub>:CO ratio) at 670 K was 9.1 on Pt/ceria and 8.6 on Pd/ceria, whereas it was 0.5 on Pd/alumina. The reason was attributed to the fact that alumina supported Pd catalyst gave poorer WGS activity than the ceria-supported one. When Pt and Pd are compared on ceria-support, Pt/ceria is found to be more selective than Pd/ceria. Pd/alumina was the least reactive and selective of the three catalysts. According to this study, the catalytic properties of Pt and Pd changed slightly when supported on ceria; Pd/ceria illustrated higher rates and selectivities than Pd/alumina. Ceria-supported catalysts have been reported to have promising effect on steam reforming of hydrocarbons (Wang and Gorte, 2002).

In another study, methane steam reforming over Ni catalyst supported on Ce-ZrO<sub>2</sub> that is the promising support of recent years, was studied at 650-900 °C in a quartz reactor system. Ni/Ce-ZrO<sub>2</sub> catalysts with different ratios of Ce-Zr and Ni/Al<sub>2</sub>O<sub>3</sub> were investigated. It was observed that the catalyst with Ce/Zr ratio of 3/1 showed the best activity and stability compared to other Ni/Ce-ZrO<sub>2</sub> samples with the Ce/Zr ratios of 1/0, 1/1, 1/3. Also the resistance toward carbon formation of Ni/Ce-ZrO<sub>2</sub> catalyst was higher

than Ni/Al<sub>2</sub>O<sub>3</sub> catalyst at the same operating conditions, because of high redox property of Ce-ZrO<sub>2</sub> support. It was also found that, Ni/Ce-ZrO<sub>2</sub> catalyst was a good methane reforming catalyst which had the high resistance toward the carbon formation. At high hydrogen appearance, Ni/Ce-ZrO<sub>2</sub> exhibited a stronger negative impact of hydrogen compared to Ni/Al<sub>2</sub>O<sub>3</sub> by the possible reduction of Ni/Ce-ZrO<sub>2</sub>. This strong negative effect of hydrogen causes a major interest for commercial applications of Ni/Ce-ZrO<sub>2</sub> catalyst (Laosiripojana, Assabumrungsant, 2005).

In the study of Souza and his coworkers (2006) it was demonstrated that, the support played a decisive role on the catalytic behaviour of catalyst. They studied autothermal reforming of methane, combining partial oxidation and reforming of methane with CO<sub>2</sub> or steam with Pt/Al<sub>2</sub>O<sub>3</sub>, Pt/ZrO<sub>2</sub> and Pt/CeO<sub>2</sub>. The Pt/ZrO<sub>2</sub> catalyst exhibited the highest initial activity but deactivated very fast due to deposition of residual carbon. Pt/CeO<sub>2</sub> catalyst showed the higher stability that is related to its coking resistance due to Pt-support interactions and the higher oxygen mobility in ceria lattice (Souza *et. al.*, 2006).

The development of more efficient catalysts to produce syngas (H<sub>2</sub> + CO) from methane is very important subject in the last decades. As much as active metal, also support plays an important role on the effectiveness of the catalyst. In one of the recent studies, lanthana- and magnesia-supported nickel catalysts with Ni-loading ranging from 10 to 30 wt.% and calcined at temperatures 1073–1273 K are prepared and tested in the catalytic partial oxidation of methane (Requies *et. al.*, 2005). Ni/MgO catalysts are more active and even more stable than the parent Ni/La<sub>2</sub>O<sub>3</sub> catalysts. The reason for the excellent performance of Ni/MgO catalyst lied in the formation of a cubic (Mg, Ni)O solid solution in which the Ni<sup>2+</sup> ions are highly stable against reduction even at temperatures as high as 1273 K. Under operation, the small fraction of nickel reduced remains highly dispersed and in close interaction with the basic MgO substrate, this structure being specially suited for syngas production from methane (Requies *et. al.*, 2005).

Metal- support interactions plays an important role on the activity of catalysts. In the study of Zhang and his colleagues (1996), the specific activity of Rh catalysts was found to strongly depend on the carrier employed to disperse the metal, decreasing in the order

yttria-stabilized zirconia (YSZ) > Al<sub>2</sub>O<sub>3</sub> > TiO<sub>2</sub> > SiO<sub>2</sub> > La<sub>2</sub>O<sub>3</sub> > MgO. The initial intrinsic activity and rate of deactivation of Rh were also found to be sensitive to the metal particle size, in the range of 1-6 nm. Both activity and rate of deactivation were found to decrease with increasing metal particle size. But the degree of these dependences was found to be largely affected by the nature of the carrier. The dependence of activity and rate of deactivation on metal particle size is likely to be related to metal - support interactions (Zhang *et al.*, 1996).

### 3. EXPERIMENTAL WORK

#### 3.1. Materials

##### 3.1.1. Chemicals

All the chemicals used for catalyst preparation are presented in Table 3.1.

Table 3.1. Chemicals used for catalyst preparation.

Chemicals	Formula	Specification	Source	MW (g/mol)
Ruthenium (III) nitrosyl nitrate	$\text{Ru}(\text{NO})(\text{NO}_3)_x(\text{OH})_y$ , $x+y=3$	1.5 %	Aldrich	318.10
Rhodium (III) nitrate solution	$\text{Rh}(\text{NO}_3)_3$	10 % (wt/wt)	Aldrich	288.92
Sodium carbonate	$\text{Na}_2\text{CO}_3$	99.9+%	Merck	105.99
Palladium (II) nitrate hydrate	$\text{Pd}(\text{NO}_3)_2 \cdot x\text{H}_2\text{O}$	Degree of hydration~2	Aldrich	230.43
Aluminum Oxide	$\alpha\text{-Al}_2\text{O}_3$	S.A =0.82 m <sup>2</sup> /g	Alfa Aesar	
Tetraammine platinum (II) nitrate	$\text{Pt}(\text{NH}_3)_4(\text{NO}_3)_2$	99.995+%	Aldrich	387.22
Titanium (IV) oxide	$\text{TiO}_2$	99 +%	Aldrich	79.87
Cerium (III) nitrate hexahydrate	$\text{Ce}(\text{NO}_3)_3 \cdot 6\text{H}_2\text{O}$	98.5+%	Aldrich	434.23
Nickel(II) nitrate hexahydrate	$\text{Ni}(\text{NO}_3)_2 \cdot 6\text{H}_2\text{O}$	99%	Merck	290.81
Aluminum Oxide	$\gamma\text{-Al}_2\text{O}_3$	99.98%	Alfa Aesar	101.96

### 3.1.2. Gases and Liquids

The gases N<sub>2</sub>, H<sub>2</sub>, He, CH<sub>4</sub>, O<sub>2</sub>, CO<sub>2</sub> and CO used in this study are supplied by Linde Gas, Istanbul, Turkey. Tables 3.1 and 3.2 show the applications and specifications of the liquids and gases used in this study

Table 3.2. Applications and specifications of the liquids used.

<b>Liquid</b>	<b>Application</b>	<b>Specification</b>
Water	Reactant, Aqueous solutions	Distilled

Table 3.3. Applications and specifications of the gases used.

<b>Gas</b>	<b>Application</b>	<b>Specification</b>
Carbon dioxide	GC Calibration	99.99%
Nitrogen	Reactant (inert)	99.998%
Methane	Reactant, GC calibration	99.7%
Dry Air	GC Calibration, Reactant	78.4%N <sub>2</sub> + 21.5%O <sub>2</sub>
Carbon monoxide	GC calibration	99.5%
Helium	Reactant (inert), GC carrier gas	99.999%
Hydrogen	Reducing agent, GC calibration	99.99%
Oxygen	GC calibration	99.99%

## 3.2. Experimental System

The experimental system used in this study can be divided mainly into three groups:

(i) Catalyst Preparation System: Incipient-to-wetness impregnation technique is used for preparation of catalysts for this study.

(ii) Catalytic Reaction System: This continuous micro-reactor flow system was modified for quartz - reactor and includes a liquid pump for water feed, mass flow controllers for inlet gases, temperature-controlled heated connecting lines and a fixed-bed flow reactor in a vertical furnace whose temperature is controlled by a programmable

temperature controller. This system is used for assessing catalytic activity and selectivity and is also suitable for future studies on reaction kinetics.

(iii) Product Analysis System: In this system, the compositions of the reactant and product gases are analyzed using two gas chromatographs which are operated in parallel.

### 3.2.1. Catalyst Preparation Systems

The system used for catalyst preparation by impregnation method included a Retsch UR1 ultrasonic mixer providing uniform mixing and contacting of the solution with the support, a vacuum pump, a Masterflex computerized-drive peristaltic pump used for addition of the solution to be impregnated, a büchner flask, a beaker and silicone tubing. The specific details are given in catalyst preparation procedure section, while the schematic representation of the impregnation method is given in Figure 3.1.

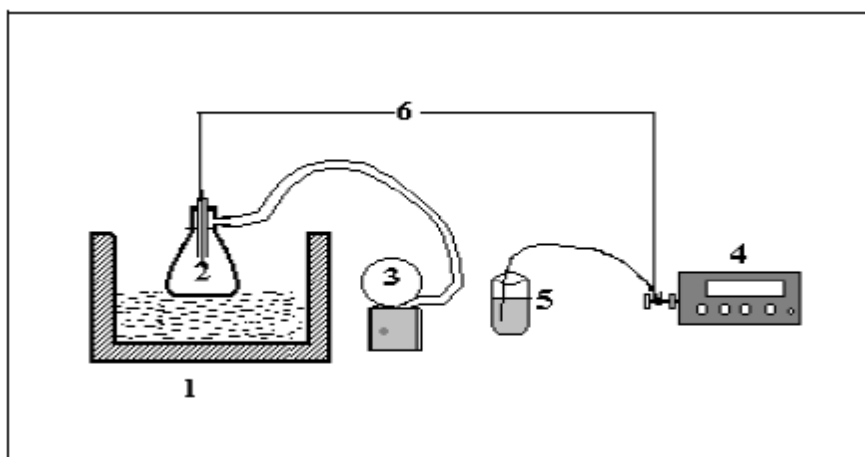


Figure 3.1. The impregnation system: 1.Ultrasonic mixer 2.Büchner flask  
3.Vacuum pump 4.Peristaltic pump 5.Beaker 6.Silicone tubing (Öztürk, 2009).

#### 3.2.1.1. $\text{CeO}_2$ Support Preparation System

$\text{CeO}_2$  support precipitated from  $\text{Ce}(\text{NO}_3)_3 \cdot 6\text{H}_2\text{O}$  by homogeneous deposition precipitation method required a stirrer, a heater circulation bath, a pH meter and a beaker.

The specific details are given in catalyst preparation procedure section, while the schematic representation of the HDP process is given in Figure 3.2.

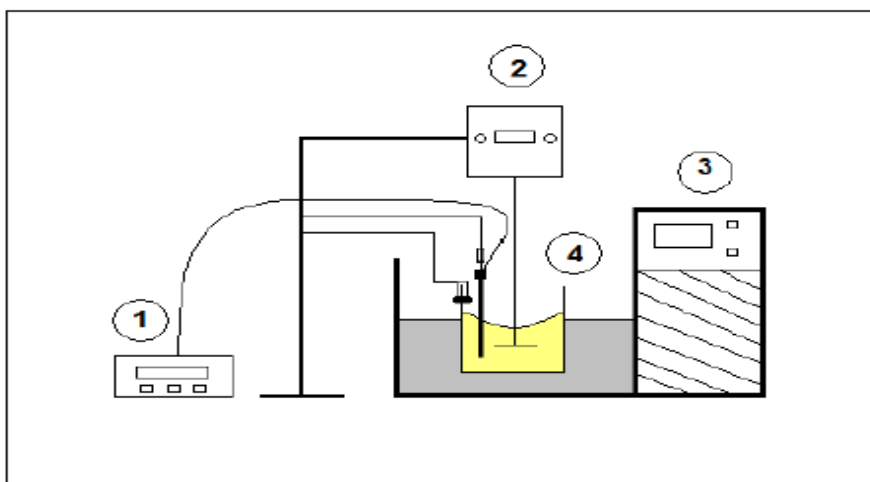


Figure 3.2. The HDP system: 1. pH meter, 2. Stirrer, 3. Heater circulation bath 4. Beaker (Güneş, 2009).

### 3.2.2. Catalytic Reaction System

The catalytic reaction system was designed and constructed in Catalyst Technology and Reaction Engineering Laboratory (CATREL). This system includes three main sections. Details and the necessary equipment for the system are presented in Section 4.

- Feed section
- Reaction section
- Product analysis section

### 3.2.3. Product Analysis System

The product mixture contains groups of species with different characteristics, i.e. methane, fixed gases like hydrogen, nitrogen, and others as carbon monoxide, carbon dioxide and water.

The reactant and product gas streams were analyzed using two different gas chromatographs: HP-Agilent 6890N and HP-Agilent 6850N. Both are temperature-controlled programmable network gas chromatographs, having thermal conductivity detectors (TCD).

Considering that all these species excluding water were analyzed quantitatively, the use of two different gas chromatographs was essential; hydrocarbons were effectively analyzed using a Porapak Q column with He carrier gas whereas quantitative detection of hydrogen and other fixed gases were analyzed using a Molecular Sieve 5A column with Ar carrier, which is easily deactivated if it is contacted with a stream containing water vapor. Thus steam existing in the product stream was removed by placing two ice cold traps. The parallel operation of these gas chromatographs was achieved by diverting the product flow with the help of three way valves. Specifications and operating conditions of both gas chromatographs are listed in Table 3.3

Table 3.4. Reactant and product gas analysis conditions.

<b>GC Parameter</b>	<b>HP Agilent 6890 N</b>	<b>HP Agilent 6850 N</b>
<b>Detector Type</b>	Thermal Conductivity	Thermal Conductivity
<b>Column Oven Temperature</b>	40°C	40°C
<b>Injector Temperature</b>	40°C	110°C
<b>TCD Temperature</b>	150°C	150°C
<b>Carrier Gas</b>	Argon	Helium
<b>Carrier Gas Flow Rate</b>	40 ml.min <sup>-1</sup>	20 ml min <sup>-1</sup>
<b>Column Packing Material</b>	Molecular Sieve 5A, 60-80 mesh	Porapak Q, 80-100 mesh
<b>Column Tubing Material</b>	Stainless Steel	Stainless Steel
<b>Column ID &amp; Length</b>	1/8" OD x 2 m	1/8" OD x 3 m
<b>Sample Loop</b>	1 ml	1 ml

### 3.3. Catalyst Preparation and Pretreatment

#### 3.3.1. Support Preparation

3.3.1.1. Alumina. The catalytic steam reforming of hydrocarbons is known to be a high-temperature reaction. Therefore, the catalyst supports should not only have high surface areas, but also possess high thermal stabilities.  $\gamma$ - $\text{Al}_2\text{O}_3$  is a commonly used support material due to its high surface area. However, it is reported to have low stability at temperatures higher than 873 K and tends to facilitate carbon formation in the presence of steam due to its high acidity. The most thermally stable version of alumina is obtained when  $\gamma$ -phase is transformed into  $\alpha$ -phase at temperatures higher than 1400 K. However, its low surface area being less than  $5 \text{ m}^2/\text{g}$ , is likely to end up with poor catalytic activities due to the low dispersion of active metals. Hence, using a support such as  $\delta$ -alumina, an intermediate phase between  $\gamma$  and  $\alpha$ , having relatively high thermal stability and an acceptable surface area is optimum in terms of obtaining efficient catalytic performance (Ma, 1995).

The support preparation procedure used in this study involved crushing and sieving  $\gamma$ - $\text{Al}_2\text{O}_3$  into 400-200  $\mu\text{m}$  (45-60 mesh) particle size and drying at 423 K for 2h followed by calcination at 1173 K for 4h in a muffle furnace. BET surface area of the  $\delta$ - $\text{Al}_2\text{O}_3$  support obtained was found as  $81.6 \text{ m}^2/\text{g}$  (Avci, 2003).

3.3.1.2. Titania. The support preparation procedure involved sieving  $\text{TiO}_2$  into 400-200  $\mu\text{m}$  (45-60 mesh) particle size and calcined 500  $^\circ\text{C}$  for 4 hours.

3.3.1.3. Ceria.  $\text{CeO}_2$  support was prepared from  $\text{Ce}(\text{NO}_3)_3 \cdot 6\text{H}_2\text{O}$ , by homogeneous precipitation method using  $\text{Na}_2\text{CO}_3$  solution in HDP system as shown in Figure 3.2. 21.7115 gr  $\text{Ce}(\text{NO}_3)_3 \cdot 6\text{H}_2\text{O}$  and 100 ml deionized water was put in a beaker and beaker was placed in HDP system in water bath at a constant temperature of 65  $^\circ\text{C}$ . The system was carried out under fully controlled pH, stirring speed and temperature. The pH was adjusted by adding aqueous  $\text{Na}_2\text{CO}_3$  solution with 2 gr  $\text{Na}_2\text{CO}_3$  and 20 ml deionized water; 3 gr  $\text{Na}_2\text{CO}_3$  and 30 ml deionized water; 4 gr  $\text{Na}_2\text{CO}_3$  and 20 ml deionized water until at a pH value of 8. Then ceria was suspended for 1 hour at a pH 8.0-8.5 in water bath at 65  $^\circ\text{C}$ .

The solution was filtered and washed with deionized water, dried 105 °C overnight and calcined 400 °C for 4 hours (Çağlayan, 2011).

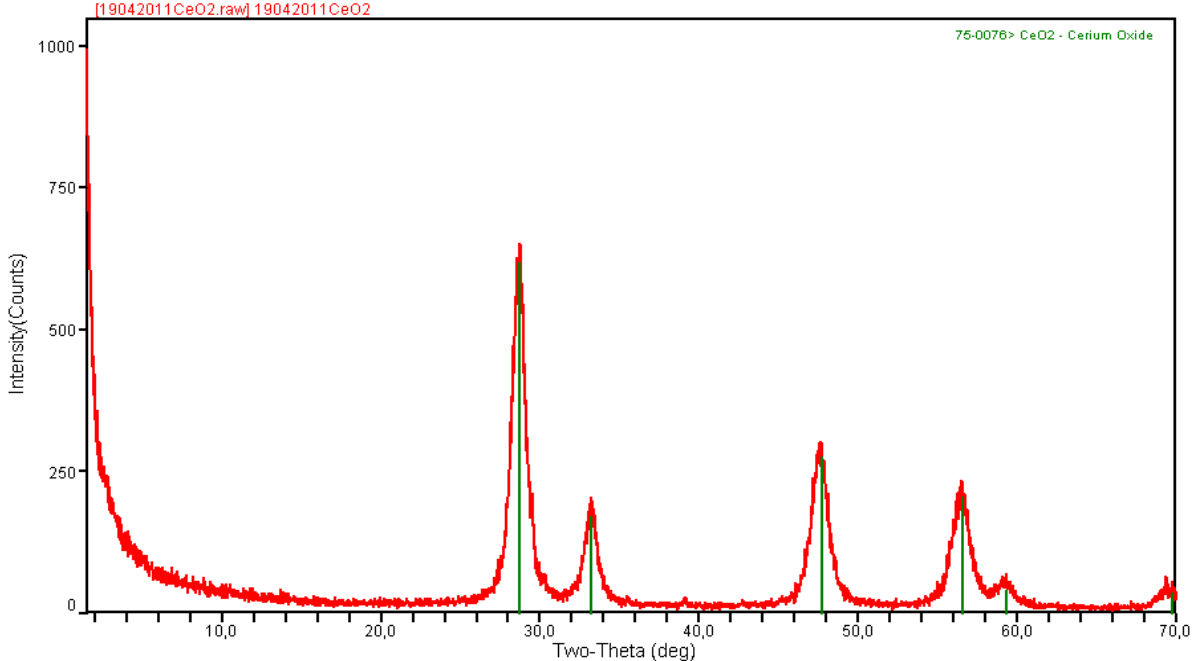


Figure 3.3. XRD Analysis of Ceria Sample-1.

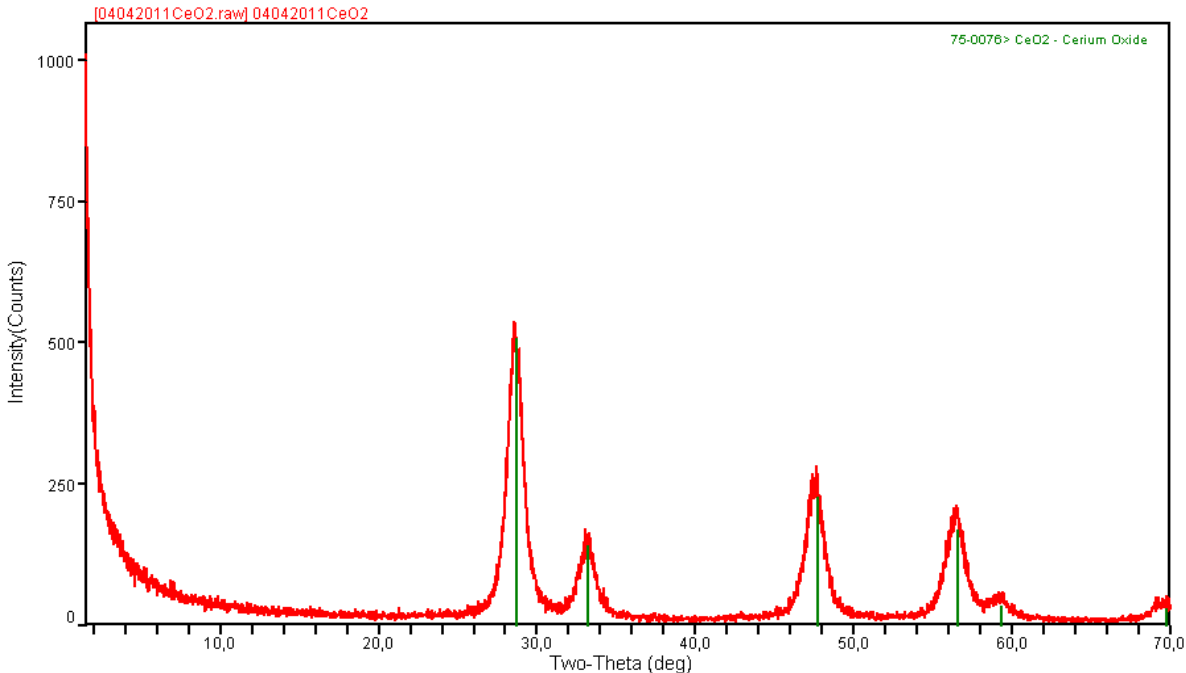


Figure 3.4. XRD Analysis of Ceria Sample-2.

The XRD analyses of the CeO<sub>2</sub> samples are illustrated in Figures 3.3 and 3.4. For all the preparations the diffraction analysis indicates the formation of one structure peak which is belong to CeO<sub>2</sub>. Therefore, the preparation procedure of the CeO<sub>2</sub> is the successful procedure.

3.3.1.4. Preparation of Ni/ $\delta$ -Al<sub>2</sub>O<sub>3</sub> Catalyst. The Ni/ $\delta$ -Al<sub>2</sub>O<sub>3</sub> catalyst (15% Ni) was prepared by the incipient-to-wetness impregnation technique using aqueous solution of Ni(NO<sub>3</sub>)<sub>2</sub>.6H<sub>2</sub>O. The aqueous solution was prepared by dissolving a calculated amount of the precursor salt in definite amounts of de-ionized water (ca. 1.1 ml solution/g support). The support,  $\delta$ -Al<sub>2</sub>O<sub>3</sub>, was placed in a Büchner flask, kept under vacuum before, during and after the addition of precursor solutions. Since trapped air in the pores of the support could prevent penetration of the solutions, vacuum pump was used to remove the trapped air and to give a uniform distribution of the active component. Thus, before impregnating the solution, the support material was mixed with ultrasonic mixer for 25 min under vacuum. A Masterflex computerized-drive peristaltic pump was used to feed the precursor solution to the vacuum flask at a rate of 0.5 mL/min via silicone tubing. The resulting thick slurry formed after ultrasonic mixing of the aqueous solution and the support under vacuum for 1.5 h was then dried overnight at 393 K and calcined at 873 K for 4 h to obtain Ni/ $\delta$ -Al<sub>2</sub>O<sub>3</sub>. Other catalaysts were also preperaed by the incipient-to-wetness impregnation technique. However, the preperation conditions that are given below in Table 3.5 and 3.6 are different from each other because of the different chemical properties.

3.3.1.5. Pretreatment of Catalysts. In order to obtain high catalytic activities, a pretreatment involving the reduction of the active metals from the oxide state, which is formed during the calcinations, to the metallic state is required prior to the reaction, since catalysts in their oxide forms are usually inactive for the reactions.

Ma (1995) has reported that during reduction, the water in the catalysts may cause premature sintering, which may lead to deactivation before the reaction. Considering these issues, the following stepwise reduction procedure was followed for the catalyst used in all of the experiments (Avci, 2003).

After placing the catalyst into the constant temperature zone of the micro-reactor, N<sub>2</sub> was allowed to flow at 50 ml/min for 10 minutes to remove oxygen from the system. The temperature was increased from room temperature to 523 K and kept constant for 15 minutes. Second step involved heating the sample from 523 K to 673 K at a rate of 10 K/min, followed by a 15 min isothermal segment. The temperature was then increased from 673 K to 1073 K at a rate of 10 K/min and finally kept constant at 1073 K for 2 h. The gas flow was switched from N<sub>2</sub> to H<sub>2</sub> and the latter was set to flow at 25 ml/min. Reduction was started at the constant temperature of 1073 K for 2 hours. After reduction, the system was allowed to cool down to ca. 523 K under N<sub>2</sub> flow at 20 ml/min. Below this temperature, the gas flow was decreased from 20 ml/min to 5 ml /min and the latter was allowed to flow at a small flow rate, e.g. 5 ml/min, overnight to sweep H<sub>2</sub> from the system prior to the tests.

Table 3.5. The Prepared Catalysts.

Cat #	Composition	Calcination	Amount of solution per unit support used for the impregnation
1	Support: %85 $\delta$ -Al <sub>2</sub> O <sub>3</sub> Metals: % 15 Ni	$\delta$ -Al <sub>2</sub> O <sub>3</sub> : 4 hrs 900 °C Ni/ $\delta$ -Al <sub>2</sub> O <sub>3</sub> : 4 hrs 600 °C	1.1 ml solution/g support (Ni Impregnation)
2	%99 $\delta$ -Al <sub>2</sub> O <sub>3</sub> , % 1 Pd	$\delta$ -Al <sub>2</sub> O <sub>3</sub> : 4 hrs 900 °C Pd/ $\delta$ -Al <sub>2</sub> O <sub>3</sub> : 4 hrs 500 °C	1.7 ml solution/g support (Pd Impregnation)
3	%98 $\delta$ -Al <sub>2</sub> O <sub>3</sub> , % 2 Pt	$\delta$ -Al <sub>2</sub> O <sub>3</sub> : 4 hrs 900 °C Pt/ $\delta$ -Al <sub>2</sub> O <sub>3</sub> : 4 hrs 500 °C	1.45 ml solution/g support (Pt Impregnation)
4	%98 $\delta$ -Al <sub>2</sub> O <sub>3</sub> , % 2 Rh	$\delta$ -Al <sub>2</sub> O <sub>3</sub> : 4 hrs 900 °C Rh/ $\delta$ -Al <sub>2</sub> O <sub>3</sub> : 4 hrs 500 °C	1.3 ml solution/g support (Rh Impregnation)
5	%98 $\delta$ -Al <sub>2</sub> O <sub>3</sub> , % 2 Ru	$\delta$ -Al <sub>2</sub> O <sub>3</sub> : 4 hrs 900 °C Ru/ $\delta$ -Al <sub>2</sub> O <sub>3</sub> : 4 hrs 500 °C	1.1 ml solution/g support (Ru Impregnation)
6	%85 TiO <sub>2</sub> , % 15 Ni	TiO <sub>2</sub> : 4 hrs 500 °C Ni/TiO <sub>2</sub> : 4 hrs 600 °C	0.4 ml solution/g support (Ni Impregnation)
7	%99 TiO <sub>2</sub> , % 1 Pd	TiO <sub>2</sub> : 4 hrs 500 °C Pd/TiO <sub>2</sub> : 4 hrs 500 °C	0.9 ml solution/g support (Pd Impregnation)
8	%98 TiO <sub>2</sub> , % 2 Pt	TiO <sub>2</sub> : 4 hrs 500 °C Pt/TiO <sub>2</sub> : 4 hrs 500 °C	0.95 ml solution/g support (Pt Impregnation)
9	%98 TiO <sub>2</sub> , % 2 Rh	TiO <sub>2</sub> : 4 hrs 500 °C Rh/TiO <sub>2</sub> : 4 hrs 500 °C	0.9 ml solution/g support (Rh Impregnation)

Table 3.6. The Prepared Catalysts cont.

Cat #	Composition	Calcination	Amount of solution per unit support used for the impregnation
10	%98 TiO <sub>2</sub> , % 2 Ru	TiO <sub>2</sub> : 4 hrs 500 °C Ru/TiO <sub>2</sub> : 4 hrs 500 °C	1.27 ml solution/g support (Ru Impregnation)
11	%85 CeO <sub>2</sub> , % 15 Ni	CeO <sub>2</sub> : 4 hrs 400 °C Ni/CeO <sub>2</sub> : 4 hrs 600 °C	0.6 ml solution/g support (Ni Impregnation)
12	%99 CeO <sub>2</sub> , % 1 Pd	CeO <sub>2</sub> : 4 hrs 400 °C Pd/CeO <sub>2</sub> : 4 hrs 500 °C	1.2 ml solution/g support (Pd Impregnation)
13	%98 CeO <sub>2</sub> , % 2 Pt	CeO <sub>2</sub> : 4 hrs 400 °C Pt/CeO <sub>2</sub> : 4 hrs 500 °C	1.2 ml solution/g support (Pt Impregnation)
14	%98 CeO <sub>2</sub> , % 2 Rh	CeO <sub>2</sub> : 4 hrs 400 °C Rh/CeO <sub>2</sub> : 4 hrs 500 °C	1.1 ml solution/g support (Rh Impregnation)
15	%98 CeO <sub>2</sub> , % 2 Ru	CeO <sub>2</sub> : 4 hrs 400 °C Ru/CeO <sub>2</sub> : 4 hrs 500 °C	1.4 ml solution/g support (Ru Impregnation)

### 3.4. Reaction Tests

#### 3.4.1. Preliminary Work

Before starting the experiments, gas chromatographs were calibrated by injecting known amounts of the species separately to the chromatographic column under the conditions given in Table 3.4 and by reading the corresponding retention time and the area under the peak calculated by computer software. Using this procedure, peak area versus volume per cent graphs, given in Appendix A, were constructed for each gas and the corresponding calibration curves were determined by linear regression.

#### 3.4.2. Blank Tests

Blank tests were conducted to ensure that the material of construction, glass-wool and  $\delta$ -alumina (used as inert material within the catalyst bed) did not interfere with the

reaction test outputs. The results indicated that these items above were inactive under the conditions used in the reaction experiments.

### **3.4.3. Steam Reforming of Methane over Studied Catalysts**

In steam reforming experiments, 225 mg of fresh catalyst was placed into the constant temperature zone of microreactor. The catalysts were pretreated through reduction as described in the previous section. The temperature of the quartz reactor was raised to the reaction temperature under inert nitrogen flow of 25 ml/min. After reaching the reaction temperature, flow was decreased and nitrogen was trapped within the reactor by diverting the flow to the bypass vent. Feed gases (methane, 15 ml/min; steam, 37.5 ml/min and nitrogen, 97.5 ml/min) were allowed to flow through the bypass vent line for 30 minutes to ensure steady-state homogeneous flow. Firstly steam and nitrogen were allowed to flow and, five minutes later, methane was allowed, to stabilize the desired steam/carbon ratio of 2.5. The reaction was started after 30 minutes by diverting the feed flow into the reactor. Product samples were collected and analyzed at 30 minute, 2 hour, 3 hour, 4 hour, 5 hour and 6 hour intervals for 6h after the initiation of the reaction.

## **3.5. Design and Construction of the System**

The microreactor flow system was designed and constructed in the laboratory with all necessary tubing and fitting materials and auxiliary units. Details of the system designed for conducting methane steam reforming and autothermal reforming experiments are presented in Figures 3.5 and 3.8.

The system consisted of three parts:

- i. Feed section
- ii. Reaction section
- iii. Feed/Product analysis section

### 3.5.1. Feed Section

The feed section was composed of mass flow controllers, 1/4", 1/8" and 1/16" OD stainless steel and brass tubes and fittings for feeding the reactants to the system. In this section, the research grades of pure CH<sub>4</sub>, O<sub>2</sub>, H<sub>2</sub>, and N<sub>2</sub> gases from pressurized cylinders were passed through brass tubes and fittings. The flow rates of the gases were controlled by Brooks 5850E mass flow controllers. The set point values of the flow controllers were adjusted by four-channel Brooks 0154 control panel. Inlet pressure to the flow controllers was 30 psi for all reaction gases, but flow rate ranges of the flow controllers were different. These ranges of the mass flow controllers were selected to provide the desired gas flow rates. The specifications of the mass flow controllers used are given in Table 3.6. The mass flow controllers were calibrated *in situ* and their calibration curves are presented in Appendix B. At the inlet and the outlet of the mass flow controllers, 1/4" stainless steel tubes were used until the primary mixing zone. On-off valves were placed after the mass flow controllers. In order to provide homogeneous mixing, the reactant gases were passed through the primary mixing region before the water feed was introduced. This primary mixing region was constructed using 1/8" stainless steel tubes. The reactant gases were passed through the heated stainless steel tubing in order to get the sufficient energy to vaporize the water. A 4 m-long heating tape was used to heat the lines and a 16-gauge wire K-type sheathed thermocouple was placed along the heated lines and connected to a temperature controller. The heating tape was covered with ceramic wool insulation to prevent heat losses. The temperature was controlled by Love Controls 16A Series controller. Water was fed to the reaction system at constant flow rates using an Agilent 1200 Isocratic HPLC pump. Distilled water was used for all experiments and it was added after all reaction gases were mixed. Water was allowed to flow through the 1/16" tube and then let into the heated tubes through which the gas mixture passed. The gas mixture and steam were mixed in a secondary mixing region. This secondary mixing region was made using 1/16" stainless steel tube, after which the diameter of connecting lines was gradually increased to 1/8" and 1/4". Gas flow was diverted using a three way valve. The flow could be sent to vent line in order to ensure the mixing of the steam and the reactant gases to get a steady flow before the reaction or it could be sent to another three way valve. This second valve was used to send the flow to the bypass line, so that feed composition could be analyzed in the gas chromatograph or to the reaction section. An on-off valve was

placed at the end of the bypass line. This valve prevented the product gases to fill the bypass line when it was closed (Şen, 2008).

Table 3.7. Specifications of the mass flow controllers.

<b>Gas Type</b>	<b>N<sub>2</sub></b>	<b>CH<sub>4</sub></b>	<b>O<sub>2</sub></b>	<b>H<sub>2</sub></b>
<b>Flow Rate Range (ml.min<sup>-1</sup>)</b>	0-200	0-100	0-100	0-100
<b>Upstream Pressure (psi)</b>	30	30	30	30
<b>Maximum Working Pressure (bar)</b>	100	100	100	100
<b>Ambient Temperature Limits (°C)</b>	5 to 65	5 to 65	5 to 65	5 to 65

### 3.5.2. Reaction Section

The reaction section was connected by 1/4" stainless steel tubes and consisted of a 2.6 cm ID x 50 cm tube furnace and 10 mm ID x 80 cm quartz fixed-bed down-flow microreactor. The reactor was longer than the furnace which facilitated the placement of the reactor in the furnace by the help of stainless steel fittings. For connecting the quartz reactor with the rest of the system through both ends of the reactor, stainless steel fittings welded to 1/4" stainless steel tubes were designed and constructed. Both fittings were identical with an inner diameter of 10 mm, an outer diameter of 22 mm and a height of 150 mm. They held the reactor tight and still, preventing any gas leak or any damages from outside (Paksoy, 2010).

The microreactor was located in the furnace controlled to  $\pm 0.5$  K sensitivity by a Shimaden FP-21 programmable temperature controller. The center of quartz microreactor was designed to be able to hold the ceramic glass wool which was used to hold the catalyst bed in fixed position. The position of the catalyst bed was adjusted to remain within the constant-temperature zone (10 cm) of tube furnace. 20-gauge wire K-type sheathed thermocouple was placed near the center of the catalyst bed just outside the microreactor wall and was connected to the temperature controller. The reactor and furnace system is presented in Figure 3.5. The spaces between the inlet of the reactor-furnace and also the outlet of the reactor-furnace were insulated using ceramic wool to prevent heat loss and maintain stable temperature profile. At the end of the reactor an on-off valve was placed and it was kept closed during feed analysis to prevent back flow of the feed mixture into the reactor (Şen, 2008).

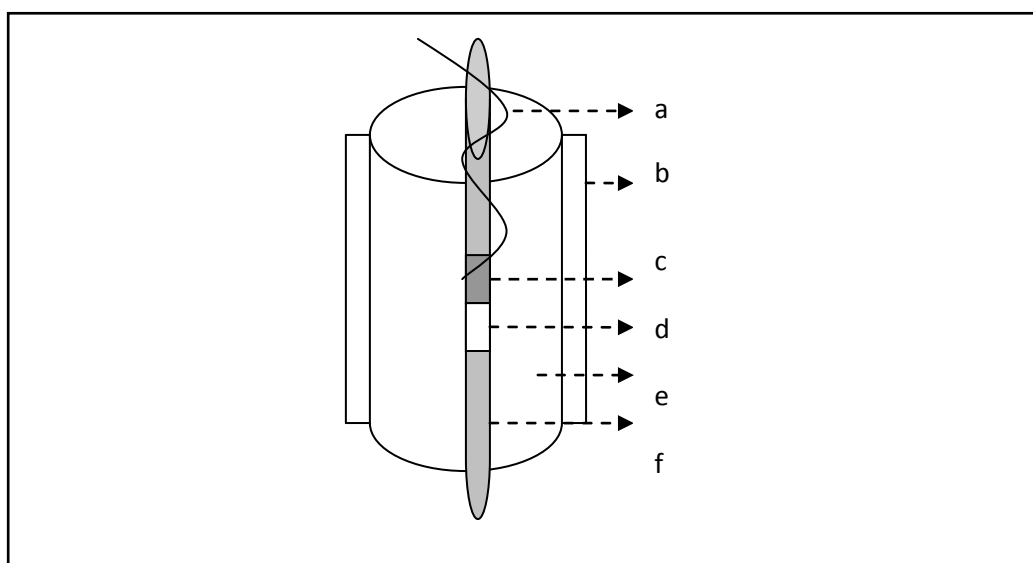


Figure 3.5. Schematic diagram of the reactor and furnace system: a. Thermocouple  
b. Ceramic wool insulation c. Catalyst d. Catalyst bed e. Furnace f. Reactor.

### 3.5.3. Feed/Product Analysis Section

The products leaving the reactor and the reactant mixtures entering the reactor were analyzed using the gas chromatographs described in Section 3.2.3. The product gas stream

leaving the microreactor was passed through an on-off valve and sent to the cold trap in order to condense the remaining water vapor before it was sent to the gas chromatograph. Cold trap included a box filled with ice and coiled tubing to increase the contact time between the gas flow and cold environment. The product or reactant gas streams were passed through the three way valve which directed the flow to either the soap bubble flow meter for measuring the flow rate or to the gas chromatograph for gas analysis. The gases entered the gas chromatograph through a 1/16" stainless steel tube, therefore, the diameter of the stainless steel connecting lines were decreased gradually from 1/4" to 1/8" and 1/16" after the last three way valve. The system with two chromatographs and all the equipments is shown in Figure 3.6 for getting data from the first GC and Figure 3.7 for getting data from the second GC. The materials used in the system are listed in Table 3.7 and the integrated reformer/reactor and gas analysis system is shown in Figure 3.8.

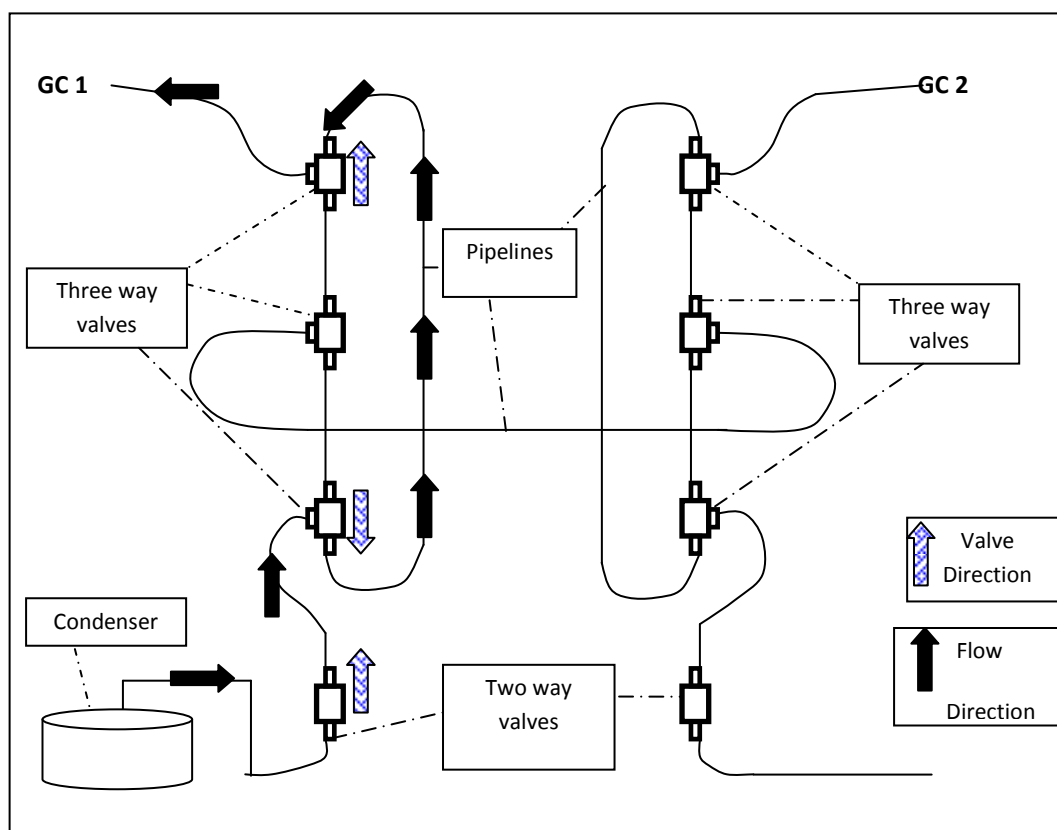


Figure 3.6. Flow routing arrangement for data analysis in GC-1.

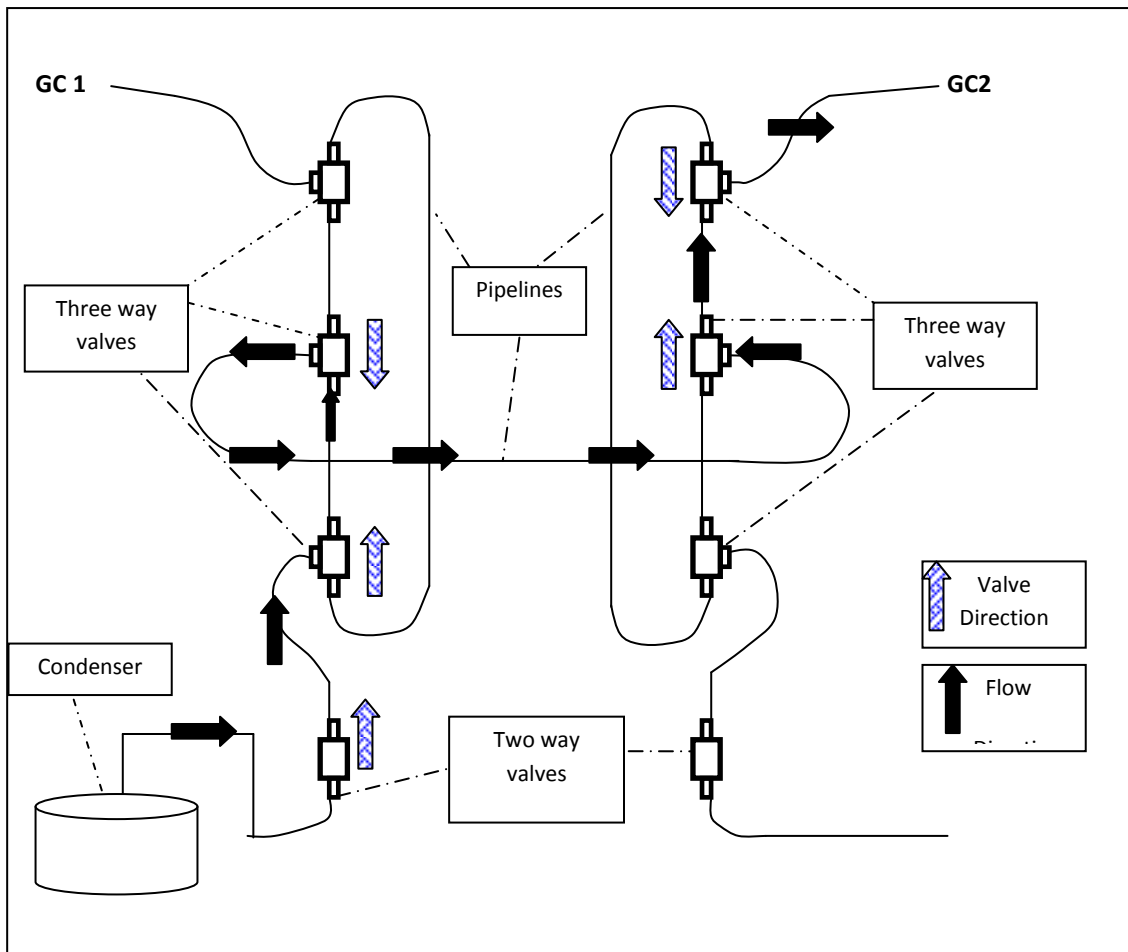


Figure 3.7. Flow routing arrangement for data analysis in GC-2.

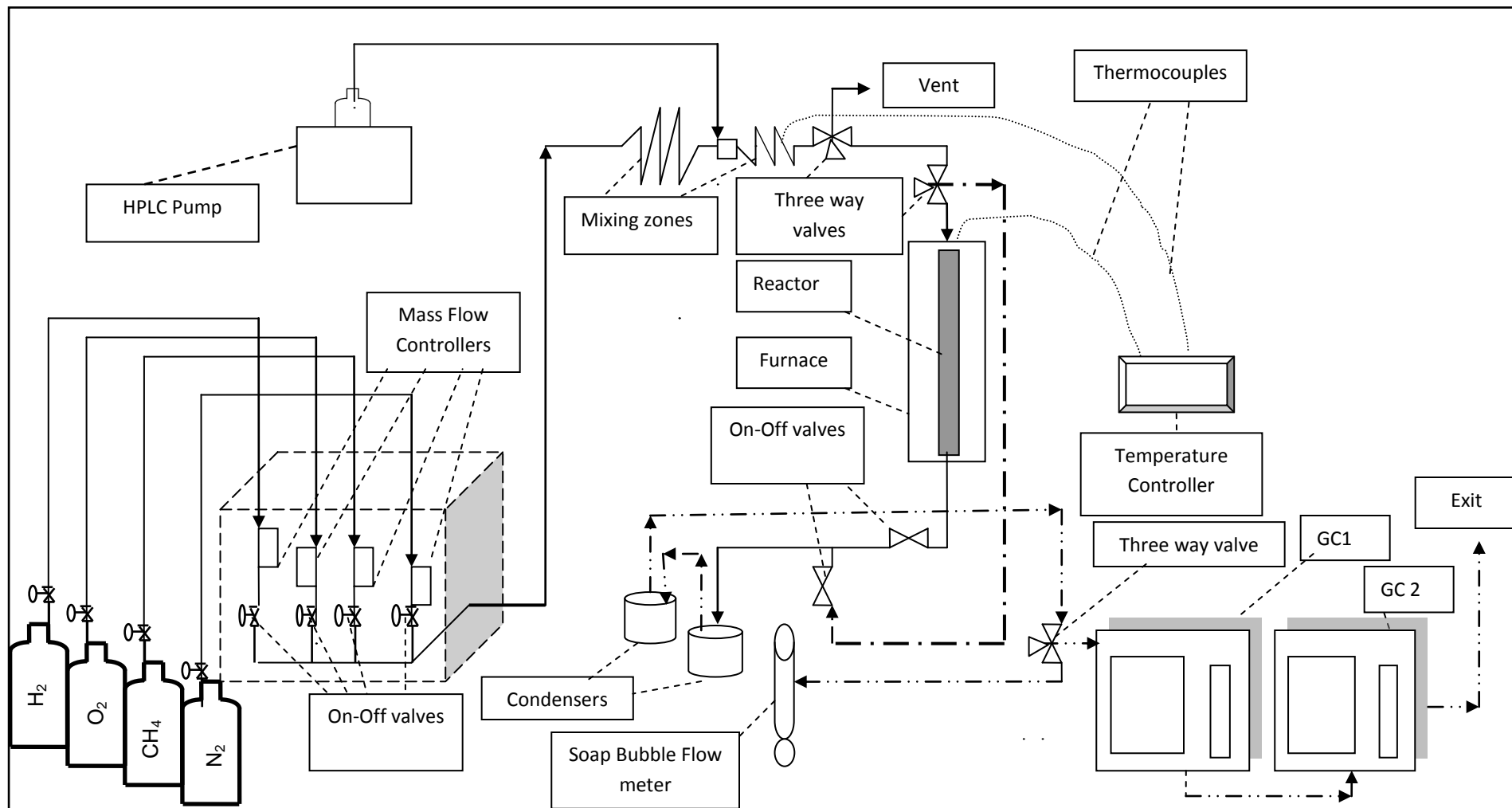


Figure 3.8. The integrated microreactor flow and product analysis system.

### 3.6. Methane Steam Reforming Experiments

In the present work, steam reforming of methane (model hydrocarbon for natural gas) was studied over 15wt% Ni/ $\delta$ -Al<sub>2</sub>O<sub>3</sub>, 1wt% Pd/ $\delta$ -Al<sub>2</sub>O<sub>3</sub>, 2wt% Pt/ $\delta$ -Al<sub>2</sub>O<sub>3</sub>, 2wt% Rh/ $\delta$ -Al<sub>2</sub>O<sub>3</sub>, 2wt% Ru/ $\delta$ -Al<sub>2</sub>O<sub>3</sub>, 15wt% Ni/TiO<sub>2</sub>, 1wt% Pd/TiO<sub>2</sub>, 2wt% Pt/TiO<sub>2</sub>, 2wt% Rh/TiO<sub>2</sub>, 2wt% Ru/TiO<sub>2</sub>, 15wt% Ni/CeO<sub>2</sub>, 1wt% Pd/CeO<sub>2</sub>, 2wt% Pt/CeO<sub>2</sub>, 2wt% Rh/TiO<sub>2</sub> and 2wt% Ru/TiO<sub>2</sub> catalysts at a steam to carbon ratio of 2.5 and temperature of 700 °C.

#### 3.6.1. Parameters of Activity

Catalyst particle size, gas space velocity and contact time are important factors which influence internal and external mass transfer resistances in a catalytic system. In previous studies and reactor systems, catalyst particles 250-344  $\mu$ m in size were found to be sufficiently small to avoid internal mass transport effects arising from pore diffusion under the reaction conditions used (Akin and Önsan, 1997). Similarly, total gas flow rates above 100 ml/min was found to minimize external heat and mass transport limitations. Therefore, catalyst particle size was chosen between 255-344  $\mu$ m and total flow rate was fixed at 150 ml/min.

In steam reforming experiments, catalyst weight was 750 mg that 225 mg of fresh catalyst and 525 mg diluents ( $\alpha$ -Al<sub>2</sub>O<sub>3</sub>). Total feed, which was set as 150 ml/min, consisted of 15 ml/min CH<sub>4</sub>, 37.5 ml/min steam and 97.5 ml/min nitrogen.

The conversion of CH<sub>4</sub> was defined and calculated as follows:

$$\text{CH}_4 \text{ conversion (\%)} = \frac{[\text{CH}_4]_{in} - [\text{CH}_4]_{out}}{[\text{CH}_4]_{in}} \times 100 \quad (3.1)$$

The amount of liquid water used in the experiments was calculated as follows:

$$V_{Li\ qui(H_2O)} = \frac{V_{St\ eat(H_2O)} \times \rho_{H_2O} \times R \times T}{MW_{H_2O} \times P} \quad (3.2)$$

where  $\rho=1000\text{ g.L}^{-1}$ ;  $P=1\text{ atm}$ ;  $R=0.082\text{ L.atm.mol}^{-1}.\text{K}^{-1}$ ;  $T=385\text{ K}$  and  $MW_{H_2O}=18\text{ g.mol}^{-1}$ .

The CO selectivity was defined and calculated as follows:

$$\text{CO selectivity (\%)} = \frac{[CO]_{out}}{[CO]_{out} + [CO_2]_{out}} \times 100 \quad (3.3)$$

## 4. RESULTS AND DISCUSSION

### 4.1. Stability Comparison of Support Performance

Figure 4.1 shows the CH<sub>4</sub> conversion over time for the Ni-based catalysts. The results show that Ni/CeO<sub>2</sub> and Ni/ $\delta$ -Al<sub>2</sub>O<sub>3</sub> illustrate stable catalytic activity for 6 hours during steam reforming. The stability decreases in the order of CeO<sub>2</sub> >  $\delta$ -Al<sub>2</sub>O<sub>3</sub> > TiO<sub>2</sub>. The beneficial effects of using ceria as a support over Ni-based catalysts are in accordance with the results reported in the literature. In the study of Laosiripojana and Assabumrungsant (2005), it was observed that the catalyst with Ce/Zr ratio of 3/1 exhibited the best activity and stability compared to other Ni/Ce-ZrO<sub>2</sub> samples with the Ce/Zr ratios of 1/0, 1/1, 1/3. Also the resistance toward carbon formation of Ni/Ce-ZrO<sub>2</sub> catalyst was higher than Ni/Al<sub>2</sub>O<sub>3</sub> catalyst at the same operating conditions, because of high redox property of Ce-ZrO<sub>2</sub> support (Laosiripojana, Assabumrungsant, 2005). Ceria-supported catalysts have a promising effect on steam reforming of hydrocarbons. Ni/CeO<sub>2</sub> exhibited higher activity than Ni/ $\delta$ -Al<sub>2</sub>O<sub>3</sub>. Ni/CeO<sub>2</sub> catalyst showed the higher stability that is related to its coking resistance due to Ni-support interactions and the higher oxygen mobility in ceria lattice.

Figure 4.2 illustrates the CH<sub>4</sub> conversion versus time graph for the Pd-based catalysts. It can be observed, compared to ceria and alumina supported ones, Pd/TiO<sub>2</sub> shows stable catalytic activity for 6 hours during steam reforming. In contrast with the other metals, the catalytic activity of TiO<sub>2</sub> based Pd catalyst is found to be higher than that of Pd/ceria and to be comparable with that of Pd/alumina. In the study of Yan and his colleagues (2003), it was found that Ni/TiO<sub>2</sub> catalyst provided long term stable catalytic activity during CO<sub>2</sub> reforming. Strong Ni/TiO<sub>x</sub> interaction and the presence of active oxygen within TiO<sub>2</sub> depressed the deposition of carbon over Ni/TiO<sub>2</sub> catalyst. Thus, this catalyst exhibited stable activity during CH<sub>4</sub>/CO<sub>2</sub> reforming (Yan *et. al*, 2003). Based on this observation, it can be deduced that metal-support interactions of Pd and TiO<sub>2</sub> causes a stable activity catalyst and also the presence of active oxygen within TiO<sub>2</sub> depress the deposition of carbon over Pd/TiO<sub>2</sub> catalyst.

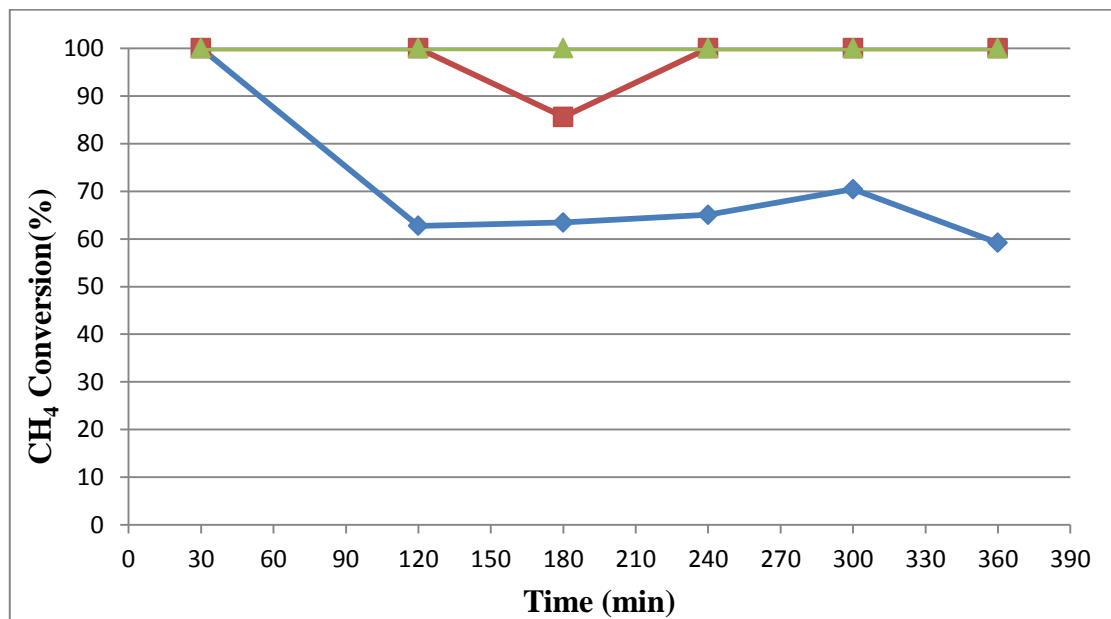


Figure 4.1 Stability Comparison of Ni-metal on Different Supports ( ◆ 15wt% Ni/TiO<sub>2</sub>

■ 15wt% Ni/ $\delta$ -Al<sub>2</sub>O<sub>3</sub> ▲ 15wt% Ni/CeO<sub>2</sub> ).

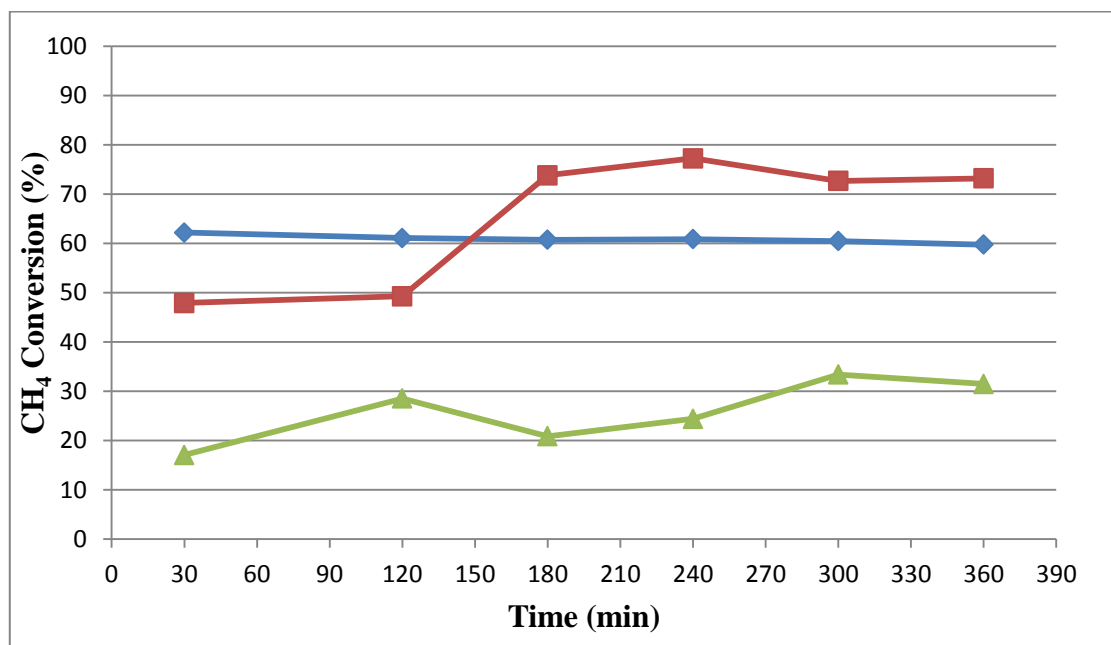


Figure 4.2 Stability Comparison of Pd-metal on Different Supports ( ◆ 1wt% Pd/TiO<sub>2</sub>

■ 1wt% Pd/ $\delta$ -Al<sub>2</sub>O<sub>3</sub> ▲ 1wt% Pd/CeO<sub>2</sub> ).

Time evolution of CH<sub>4</sub> conversion over Pt-based catalysts is given in Figure 4.3. It can be observed that Pt/ $\delta$ -Al<sub>2</sub>O<sub>3</sub> exhibited significantly higher activity than Pt/CeO<sub>2</sub> and Pt/TiO<sub>2</sub>. However Pt/ $\delta$ -Al<sub>2</sub>O<sub>3</sub> did not exhibit stability during the six hours steam reforming test; some fluctuations. Pt/TiO<sub>2</sub> gave lower catalytic activity than Pt/ $\delta$ -Al<sub>2</sub>O<sub>3</sub> and Pt/CeO<sub>2</sub>, but it exhibited higher stability than CeO<sub>2</sub> and  $\delta$ -Al<sub>2</sub>O<sub>3</sub>.

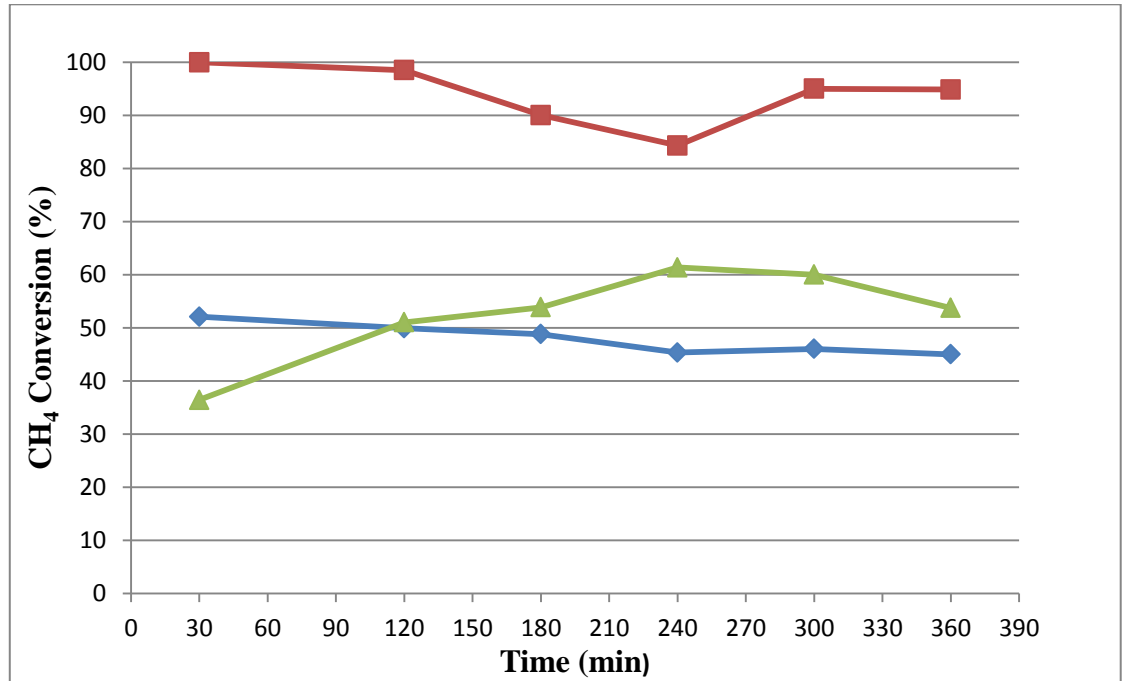


Figure 4.3 Stability Comparison of Pt-metal on Different Supports ( —◆— 2wt% Pt/TiO<sub>2</sub> —■— 2wt% Pt/ $\delta$ -Al<sub>2</sub>O<sub>3</sub> —▲— 2wt% Pt/CeO<sub>2</sub>).

Figure 4.4 shows the effects of different supports on Ru-catalyzed methane steam reforming during the reaction period studied. It can be observed that both CeO<sub>2</sub> and TiO<sub>2</sub> supported catalysts exhibited good stability. Activities of these catalysts are found to be better than that of Ru/ $\delta$ -Al<sub>2</sub>O<sub>3</sub>, which is more notable after 2h of the start-up of the reaction. The stability of  $\delta$ -Al<sub>2</sub>O<sub>3</sub> was worse than the other two catalysts. Studies in the literature also report that Ru has a good metal – support interaction with CeO<sub>2</sub>; the order of catalytic activity for CO<sub>2</sub>-CH<sub>4</sub> reforming is reported as Ru/TiO<sub>2</sub> > Ru/Al<sub>2</sub>O<sub>3</sub>  $\geq$  Ru/C (Bradford and Vannice, 1999).

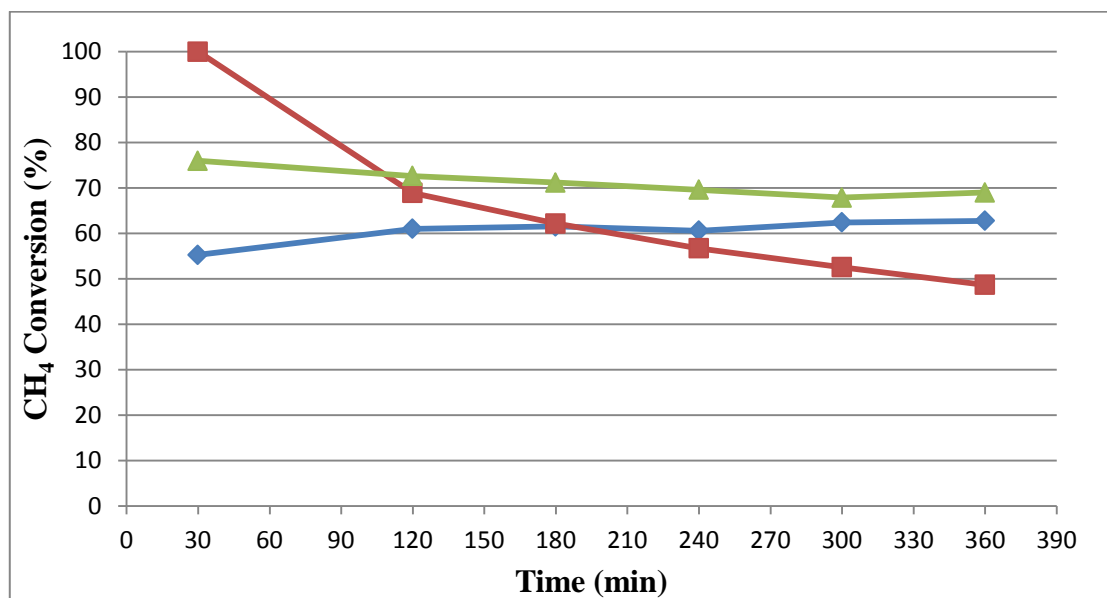


Figure 4.4 Stability Comparison of Ru-metal on Different Supports ( —◆— 2wt% Ru/TiO<sub>2</sub>

—■— 2wt% Ru/ $\delta$ -Al<sub>2</sub>O<sub>3</sub> —▲— 2wt% Ru/CeO<sub>2</sub> ).

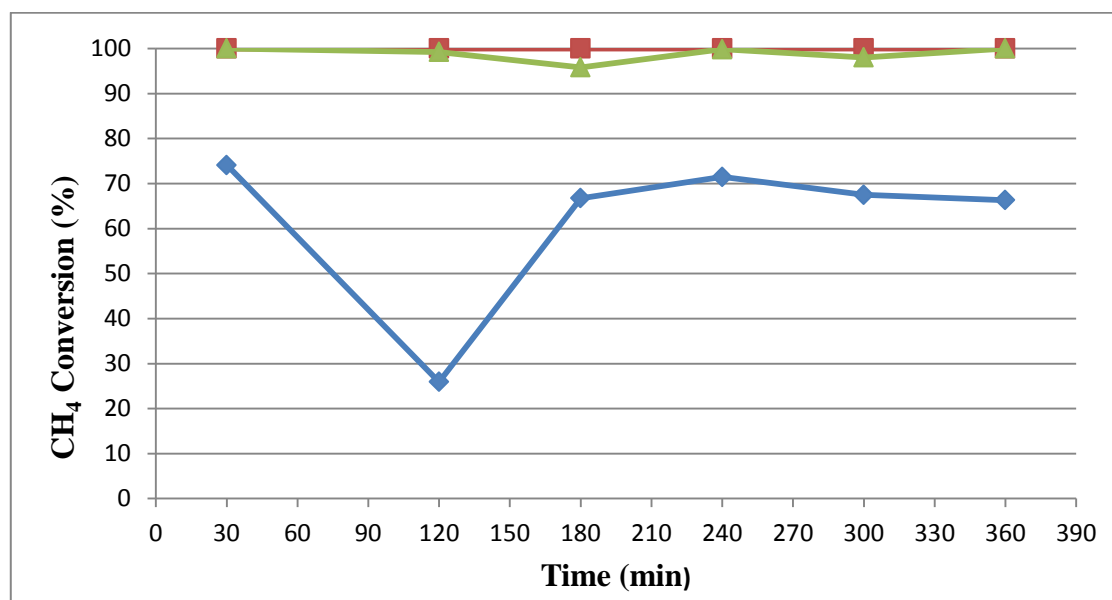


Figure 4.5 Stability Comparison of Rh-metal on Different Supports ( —◆— 2wt% Rh/TiO<sub>2</sub>

—■— 2wt% Rh/ $\delta$ -Al<sub>2</sub>O<sub>3</sub> —▲— 2wt% Rh/CeO<sub>2</sub> ).

Figure 4.5 demonstrates CH<sub>4</sub> conversion versus time for the Rh-based catalysts. Compared with the other metals, Rh gave the highest methane conversion regardless of the nature of the support, which can be attributed to the better dispersion characteristics of Rh. The activity of Rh catalysts showed some dependency on the support, which decreased in the order  $\delta$ -Al<sub>2</sub>O<sub>3</sub> > CeO<sub>2</sub> > TiO<sub>2</sub> as illustrated in Figure 4.5. Finally, it can be noted that  $\delta$ -Al<sub>2</sub>O<sub>3</sub> and CeO<sub>2</sub> supports exhibited higher stability than the TiO<sub>2</sub> support. The activity comparison is found to be similar by the results of Zhang and his colleagues (1996), who stated that Al<sub>2</sub>O<sub>3</sub>-support has higher activity than TiO<sub>2</sub>-support. The specific activity of Rh catalysts was found to strongly depend on the carrier employed to disperse the metal, decreasing in the order yttria-stabilized zirconia (YSZ) > Al<sub>2</sub>O<sub>3</sub> > TiO<sub>2</sub> > SiO<sub>2</sub> > La<sub>2</sub>O<sub>3</sub> > MgO. Metal-support interactions played an important role on the activity of catalysts (Zhang *et al.*, 1996). The activities of Rh-based catalysts reported in this study are found to be comparable also with the results of Ruckenstein and Wang (1999). They reported that, the reducible oxides are, in general, not suitable supports for rhodium in partial oxidation of methane. A possible reason was that the suboxide generated via the reduction of the reducible oxides migrated onto the surface of the metal particles, decreasing the number of active rhodium sites and hence the catalytic activity and promoting the combustion reaction. In their study, 1% Rh/ $\gamma$ -Al<sub>2</sub>O<sub>3</sub> exhibited approximately 80% CH<sub>4</sub> conversion and showed stability from 10 hours to 100 hour. 1% Rh/TiO<sub>2</sub> showed very low methane conversion under 10% and 1% Rh/CeO<sub>2</sub> showed stability from 6 hour to 14 hour and showed approximately 60% CH<sub>4</sub> conversion. As a result, the support activity decreased in the order of  $\gamma$ -Al<sub>2</sub>O<sub>3</sub> > CeO<sub>2</sub> > TiO<sub>2</sub> (Ruckenstein and Wang, 1999).

The discussions drawn for different catalysts can also be used to provide insight into the comparison of catalytic activities which are given for TiO<sub>2</sub>,  $\delta$ -Al<sub>2</sub>O<sub>3</sub> and CeO<sub>2</sub> supported catalysts in Tables 4.1, 4.2 and 4.3, respectively. Based on the results presented, activities of the metals are found to decrease in the order Rh > Ru > Pd > Ni > Pt for TiO<sub>2</sub>, Ni = Rh > Pt > Pd > Ru for  $\delta$ -Al<sub>2</sub>O<sub>3</sub> and Ni = Rh > Ru > Pt > Pd for CeO<sub>2</sub>.

Table 4.1 Activity Performance of TiO<sub>2</sub> Supported Catalysts.

<b>Support- TiO<sub>2</sub></b>	<b>CH<sub>4</sub> Conversion at 360 min (%)</b>
15wt% Ni/TiO <sub>2</sub>	59.20
1wt% Pd/TiO <sub>2</sub>	59.74
2wt% Pt/TiO <sub>2</sub>	45.01
2wt% Ru/TiO <sub>2</sub>	62.76
2wt% Rh/TiO <sub>2</sub>	66.32

Table 4.2 Activity Performance of  $\delta$ -Al<sub>2</sub>O<sub>3</sub> Supported Catalysts.

<b>Support-<math>\delta</math>-Al<sub>2</sub>O<sub>3</sub></b>	<b>CH<sub>4</sub> Conversion at 360 min (%)</b>
15wt% Ni/ $\delta$ -Al <sub>2</sub> O <sub>3</sub>	100.00
1wt% Pd/ $\delta$ -Al <sub>2</sub> O <sub>3</sub>	73.18
2wt% Pt/ $\delta$ -Al <sub>2</sub> O <sub>3</sub>	94.88
2wt% Ru/ $\delta$ -Al <sub>2</sub> O <sub>3</sub>	48.69
2wt% Rh/ $\delta$ -Al <sub>2</sub> O <sub>3</sub>	100.00

Table 4.3 Activity Performance of CeO<sub>2</sub> Supported Catalysts.

<b>Support- CeO<sub>2</sub></b>	<b>CH<sub>4</sub> Conversion at 360 min (%)</b>
15wt% Ni/CeO <sub>2</sub>	100.00
1wt% Pd/CeO <sub>2</sub>	31.48
2wt% Pt/CeO <sub>2</sub>	53.76
2wt% Ru/CeO <sub>2</sub>	69.00
2wt% Rh/CeO <sub>2</sub>	100.00

## 4.2. CO Selectivity Comparison of Support Performance

Evolution of CO selectivity with time for the Ni-based catalysts is given in Figure 4.6. The results show that Ni/TiO<sub>2</sub> exhibited no CO selectivity within the first 2 hours. CO was formed starting with second hour and its selectivity increased significantly at the third hour as shown in Figure 4.6. Ni/CeO<sub>2</sub> exhibited the best stability for CO selectivity during 6 hours. At third hour  $\delta$ -Al<sub>2</sub>O<sub>3</sub> exhibited 100% performance for CO selectivity, but didn't show stability as the CeO<sub>2</sub> supported catalyst. These results are also consistent with the CH<sub>4</sub> conversion results that gave stability decrease in the order of CeO<sub>2</sub> >  $\delta$ -Al<sub>2</sub>O<sub>3</sub> > TiO<sub>2</sub>.

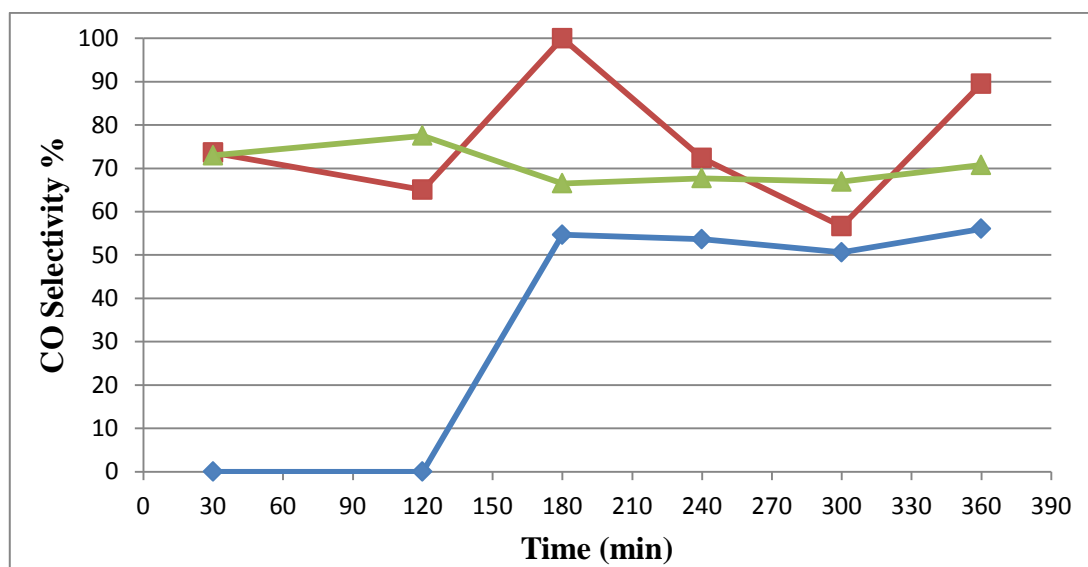


Figure 4.6 CO Selectivity % of Ni-metal on Different Supports for 6 hr ( ◆ 15wt% Ni/TiO<sub>2</sub> ■ 15wt% Ni/ $\delta$ -Al<sub>2</sub>O<sub>3</sub> ▲ 15wt% Ni/CeO<sub>2</sub> ).

Figure 4.7 gives CO selectivity versus time graph for the Pd-based catalysts. It is found that, Pd/CeO<sub>2</sub> exhibited no CO selectivity and produced CO<sub>2</sub>. The reason of such a result can be explained by the higher oxygen mobility in the ceria lattice, as a result of which CO molecules are converted to CO<sub>2</sub>. This observation is also consistent the results of Wang and Gorte (2002), in which they carried out hydrocarbon steam reforming on three different

catalysts, namely Pd/ceria, Pt/ceria and Pd/alumina. They reported that Pd/Ceria had the property of higher rates and selectivities in steam reforming of hydrocarbons when compared to Pd/Alumina, and product selectivity, expressed as molar CO<sub>2</sub>:CO ratio at 670 K, was found to be 9.1 on Pt/ceria and 8.6 on Pd/ceria (Wang and Gorte, 2002). The same study showed that CO<sub>2</sub>:CO ratio at 670 K was 0.5 on Pd/alumina. This last finding can explain the higher CO selectivity of Pd/ $\delta$ -Al<sub>2</sub>O<sub>3</sub> among Pd/TiO<sub>2</sub>, which is due to the poor WGS activity of the former support.

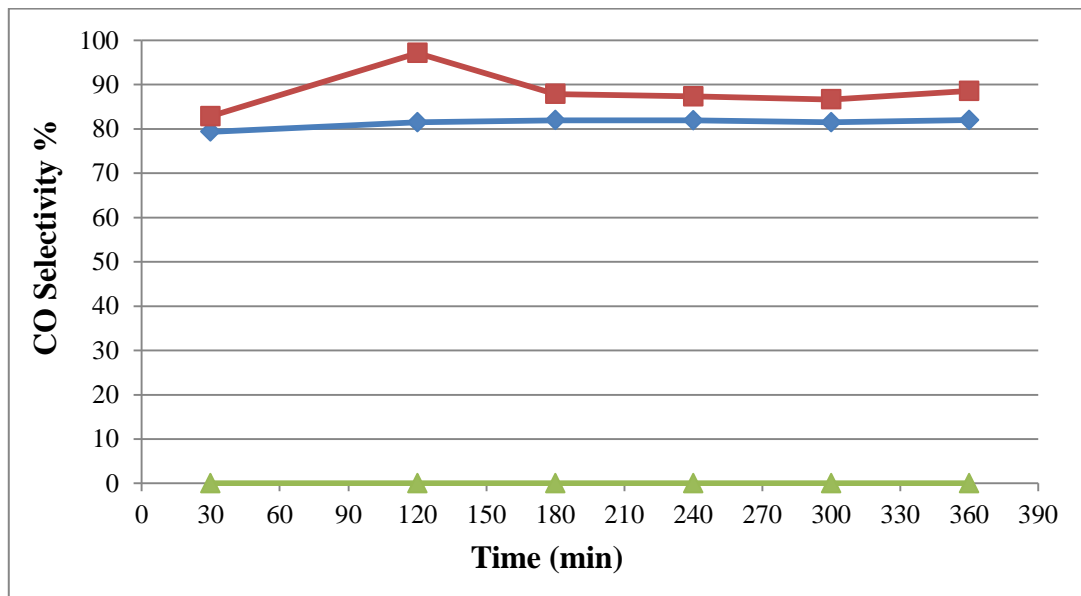


Figure 4.7 CO Selectivity % of Pd-metal on Different Supports for 6 hr ( ◆ 1wt% Pd/TiO<sub>2</sub> ■ 1wt% Pd/  $\delta$ -Al<sub>2</sub>O<sub>3</sub> ▲ 1wt% Pd/CeO<sub>2</sub> ).

Figure 4.8 gives the relation of CO selectivity and time for Pt-based catalysts. The results show that Pt/TiO<sub>2</sub> exhibited higher stability than Pt/ $\delta$ -Al<sub>2</sub>O<sub>3</sub> and Pt/CeO<sub>2</sub>, but Pt/ $\delta$ -Al<sub>2</sub>O<sub>3</sub> gave higher CO selectivities. Pt/TiO<sub>2</sub> can be considered as a good steam reforming due to its stable behavior.

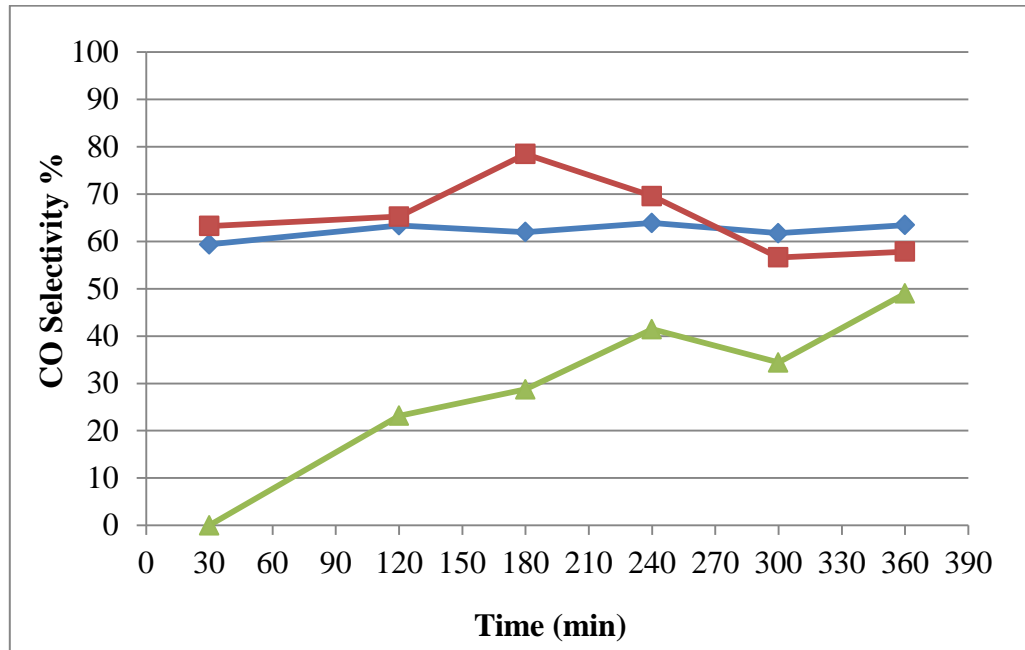


Figure 4.8 CO Selectivity % of Pt-metal on Different Supports for 6 hr ( —◆— 2wt% Pt/TiO<sub>2</sub> —■— 2wt% Pt/ $\delta$ -Al<sub>2</sub>O<sub>3</sub> —▲— 2wt% Pt/CeO<sub>2</sub>).

Figure 4.9 gives CO selectivity-time relationship for the Ru-based catalysts. It can be observed that Ru/TiO<sub>2</sub> exhibited slightly better stability than Ru/ $\delta$ -Al<sub>2</sub>O<sub>3</sub> and Ru/CeO<sub>2</sub>, and Ru/CeO<sub>2</sub> gave lower CO selectivity compared to the other Ru-based catalysts most likely due to the higher oxygen mobility in the ceria lattice. Considering its stable and CO selective behaviors, Ru/TiO<sub>2</sub> can be considered as a candidate for methane steam reforming. It is also worth noting that Pt and Ru presented similar trends in terms of CO selectivity.

CO selectivity-time graphs for the Rh-based catalysts are given in Figure 4.10. It can be noted that, Rh/ $\delta$ -Al<sub>2</sub>O<sub>3</sub> exhibited higher CO selectivity than Rh/CeO<sub>2</sub> and Rh/TiO<sub>2</sub>, which is more visible 3 h after the start-up of the reaction. This result is consistent with the order of supports in the context of methane conversion (Figure 4.5). The findings indicate that Rh has stronger metal-support interactions with  $\delta$ -Al<sub>2</sub>O<sub>3</sub>. Apart from these results, the order between Rh/CeO<sub>2</sub> and Rh/TiO<sub>2</sub> is in accordance with the literature; Ruckenstein and Wang (1999) stated that Rh/CeO<sub>2</sub> exhibited higher CO selectivity than Rh/TiO<sub>2</sub> during the partial oxidation reaction.

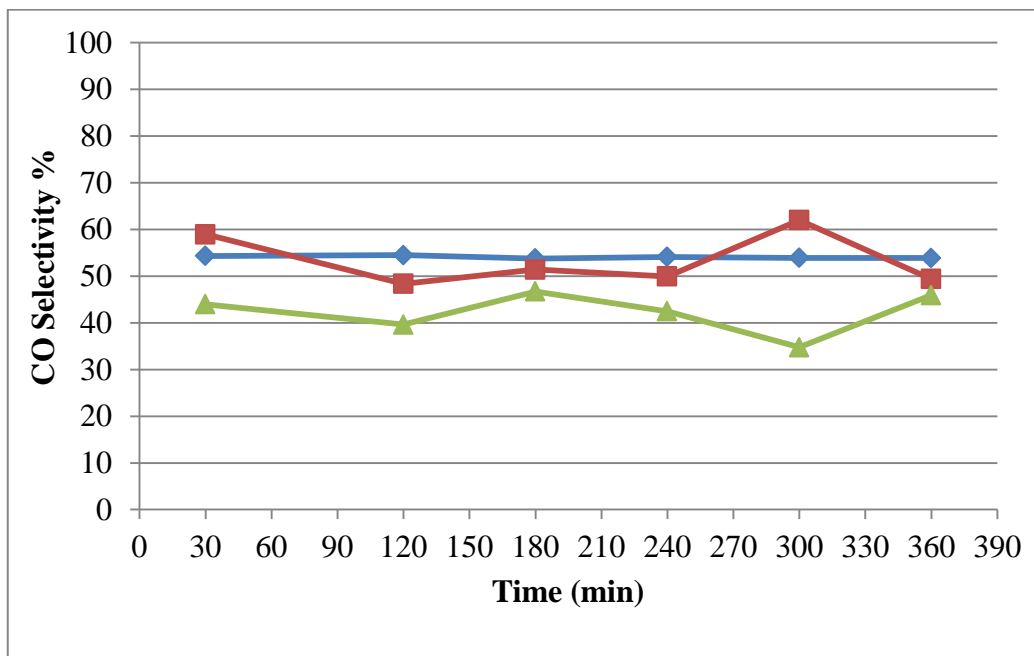


Figure 4.9 CO Selectivity % of Ru-metal on Different Supports for 6 hr ( ◆ 2wt% Ru/TiO<sub>2</sub>

■ 2wt% Ru/ $\delta$ -Al<sub>2</sub>O<sub>3</sub> ▲ 2wt% Ru/CeO<sub>2</sub>).

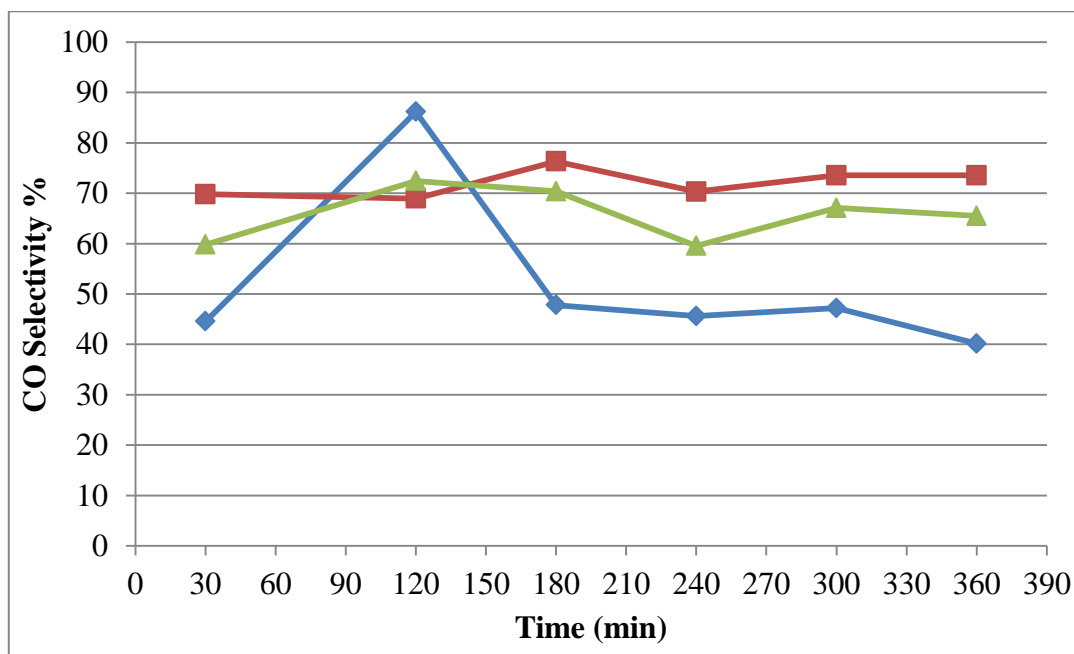


Figure 4.10 CO Selectivity % of Rh-metal on Different Supports for 6 hr ( ◆ 2wt% Rh/TiO<sub>2</sub>

■ 2wt% Rh/ $\delta$ -Al<sub>2</sub>O<sub>3</sub> ▲ 2wt% Rh/CeO<sub>2</sub>).

The results stated above for different catalysts can also be used to provide insight into the comparison of CO selectivities which are given for TiO<sub>2</sub>,  $\delta$ -Al<sub>2</sub>O<sub>3</sub> and CeO<sub>2</sub> supported catalysts in Tables 4.4, 4.5 and 4.6, respectively. Based on the results presented, CO selectivities of the metals are found to decrease in the order Pd > Pt > Ni > Ru > Rh for TiO<sub>2</sub>, Ni > Pd > Rh > Pt > Ru for  $\delta$ -Al<sub>2</sub>O<sub>3</sub> and Ni > Rh > Pt > Ru > Pd for CeO<sub>2</sub>.

Table 4.4 CO Selectivity % of TiO<sub>2</sub>-Supported Catalysts at 360 min.

<b>Support- TiO<sub>2</sub></b>	<b>CO Selectivity % at 360 min</b>
15wt% Ni/TiO <sub>2</sub>	56.01
1wt% Pd/TiO <sub>2</sub>	82.00
2wt% Pt/TiO <sub>2</sub>	63.47
2wt% Ru/TiO <sub>2</sub>	53.87
2wt% Rh/TiO <sub>2</sub>	40.13

Table 4.5 CO Selectivity % of  $\delta$ -Al<sub>2</sub>O<sub>3</sub>-Supported Catalysts at 360 min.

<b>Support-<math>\delta</math>-Al<sub>2</sub>O<sub>3</sub></b>	<b>CO Selectivity % at 360 min</b>
15wt% Ni/ $\delta$ -Al <sub>2</sub> O <sub>3</sub>	89.51
1wt% Pd/ $\delta$ -Al <sub>2</sub> O <sub>3</sub>	88.56
2wt% Pt/ $\delta$ -Al <sub>2</sub> O <sub>3</sub>	57.85
2wt% Ru/ $\delta$ -Al <sub>2</sub> O <sub>3</sub>	49.37
2wt% Rh/ $\delta$ -Al <sub>2</sub> O <sub>3</sub>	73.54

Table 4.6 CO Selectivity % of CeO<sub>2</sub>-Supported Catalysts at 360 min.

<b>Support- CeO<sub>2</sub></b>	<b>CO Selectivity % at 360 min</b>
15wt% Ni/CeO <sub>2</sub>	70.77
1wt% Pd/CeO <sub>2</sub>	0
2wt% Pt/CeO <sub>2</sub>	48.97
2wt% Ru/CeO <sub>2</sub>	45.94
2wt% Rh/CeO <sub>2</sub>	65.47

Metal-support interactions are believed to affect the CO selectivity of the Ni-catalysts. When 6 h data are compared, the CO selectivity property decreased in the order  $\delta$ -Al<sub>2</sub>O<sub>3</sub> > CeO<sub>2</sub> > TiO<sub>2</sub> as illustrated Table 4.4, 4.5 and 4.6. Ru and Pt showed similar trends for CO selectivity, which decreases in the order TiO<sub>2</sub> >  $\delta$ -Al<sub>2</sub>O<sub>3</sub> > CeO<sub>2</sub>. Pd shows the weakest CO selectivity property on the CeO<sub>2</sub> support as Ru and Pt. Rh catalysts gave similar CO selectivity trends with the Ni-based ones. In these catalysts, CO selectivity decreases in the order  $\delta$ -Al<sub>2</sub>O<sub>3</sub> > CeO<sub>2</sub> > TiO<sub>2</sub>.

## 5. CONCLUSIONS AND RECOMMENDATIONS

### 5.1. Conclusions

The major conclusions that can be drawn from this study can be outlined as follows:

- Use of ceria for supporting Ni is found to have promising effect on steam reforming of methane. It showed higher activity than Ni/ $\delta$ -Al<sub>2</sub>O<sub>3</sub> as well as higher stability that is related to its coking resistance due to Ni-support interactions and the higher oxygen mobility in the ceria lattice. The stability decreased in the order of Ni/CeO<sub>2</sub> > Ni/ $\delta$ -Al<sub>2</sub>O<sub>3</sub> > Ni/TiO<sub>2</sub>. The beneficial effects of ceria led to higher CO selectivities over Ni; for CeO<sub>2</sub> supported catalysts, selectivities are found to follow the decreasing order of Ni > Rh > Pt > Ru > Pd.
- Among the Pd-based catalysts tested, Pd/TiO<sub>2</sub> showed more stable and active performance compared to CeO<sub>2</sub> and more stable compared to  $\delta$ -Al<sub>2</sub>O<sub>3</sub>. The superior performance brought by using TiO<sub>2</sub> is believed to be due to the interactions between Pd and TiO<sub>2</sub> and the presence of active oxygen within TiO<sub>2</sub> that depresses carbon deposition over Pd/TiO<sub>2</sub> catalyst. In terms of CO selectivity, Pd/ $\delta$ -Al<sub>2</sub>O<sub>3</sub> is found to be better than Pd/TiO<sub>2</sub>.
- As in the case of Pd, Pt/TiO<sub>2</sub> demonstrated stable behavior within the reaction period. However Pt/ $\delta$ -Al<sub>2</sub>O<sub>3</sub> exhibited higher activity and selectivity.
- Ru/CeO<sub>2</sub> and Ru/TiO<sub>2</sub> catalysts exhibited good stability over the reaction period. Activities of these catalysts are found to be better than that of Ru/ $\delta$ -Al<sub>2</sub>O<sub>3</sub>. Ru/CeO<sub>2</sub> gave lower CO selectivity compared to the other Ru-based catalysts most likely due to the higher oxygen mobility in the ceria lattice. Considering its stable and CO selective behaviors, Ru/TiO<sub>2</sub> can be considered as a candidate for methane steam reforming.
- Methane conversions obtained over Rh-based catalysts decreased in the order  $\delta$ -Al<sub>2</sub>O<sub>3</sub> > CeO<sub>2</sub> > TiO<sub>2</sub>.  $\delta$ -Al<sub>2</sub>O<sub>3</sub> and CeO<sub>2</sub> supports exhibited higher stability than TiO<sub>2</sub>. CO

selectivity of Rh/ $\delta$ -Al<sub>2</sub>O<sub>3</sub> is found to be higher than those of Rh/CeO<sub>2</sub> and Rh/TiO<sub>2</sub>. Rh is believed to make positive interactions with  $\delta$ -Al<sub>2</sub>O<sub>3</sub> under the reaction conditions tested.

- Activities (methane conversions) of the metals are found to decrease in the order Rh > Ru > Pd > Ni > Pt for TiO<sub>2</sub>, Ni = Rh > Pt > Pd > Ru for  $\delta$ -Al<sub>2</sub>O<sub>3</sub> and Ni = Rh > Ru > Pt > Pd for CeO<sub>2</sub>.
- CO selectivities of the metals are found to decrease in the order Pd > Pt > Ni > Ru > Rh for TiO<sub>2</sub>, Ni > Pd > Rh > Pt > Ru for  $\delta$ -Al<sub>2</sub>O<sub>3</sub> and Ni > Rh > Pt > Ru > Pd for CeO<sub>2</sub>.

## 5.2. Recommendations

Under the light of the results of the present work, the following studies are recommended:

- Experiments can be repeated by changing the catalyst preparation method on the same catalysts.
- The reaction temperature can be changed to observe the behaviours of catalysts on different temperatures to make comparison.
- Different supports as MgO and La<sub>2</sub>O<sub>3</sub> can be tested under the same experimental parameters.

## APPENDIX A: CALIBRATION CURVES OF THE GAS CHROMATOGRAPH

Calibration curves of the gas chromatograph used in the experiments are given below.

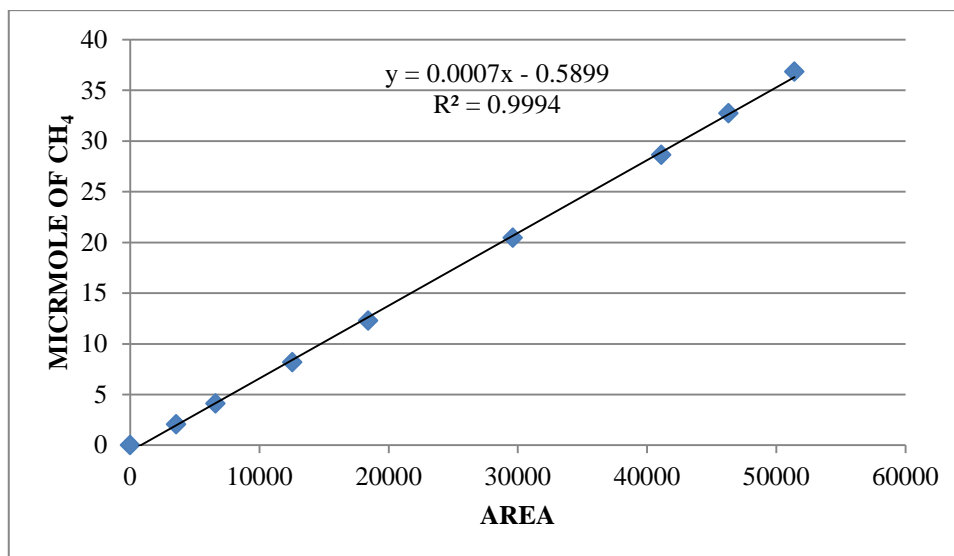


Figure A.1. Calibration curve of methane

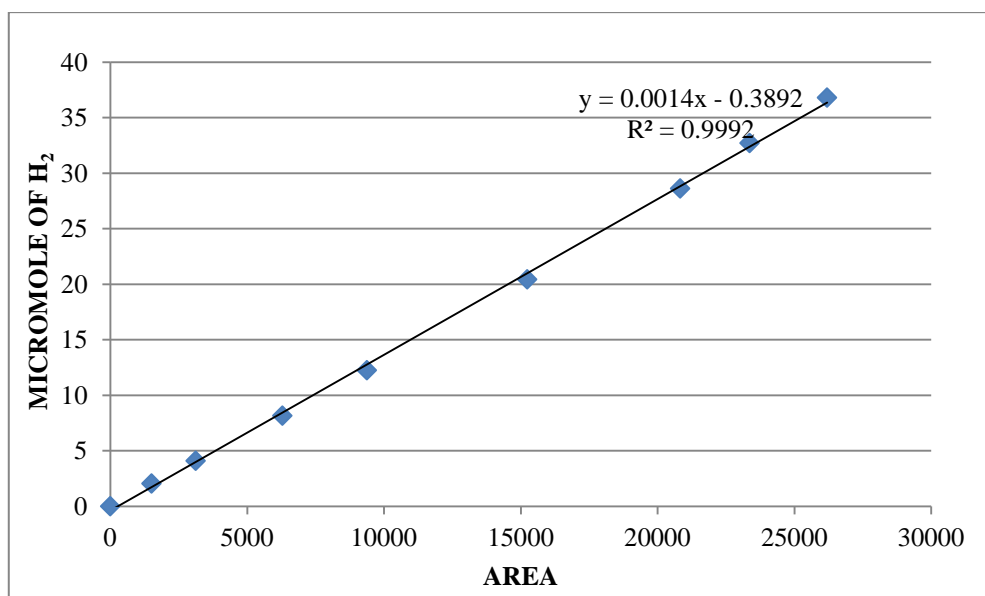


Figure A.2. Calibration curve of hydrogen

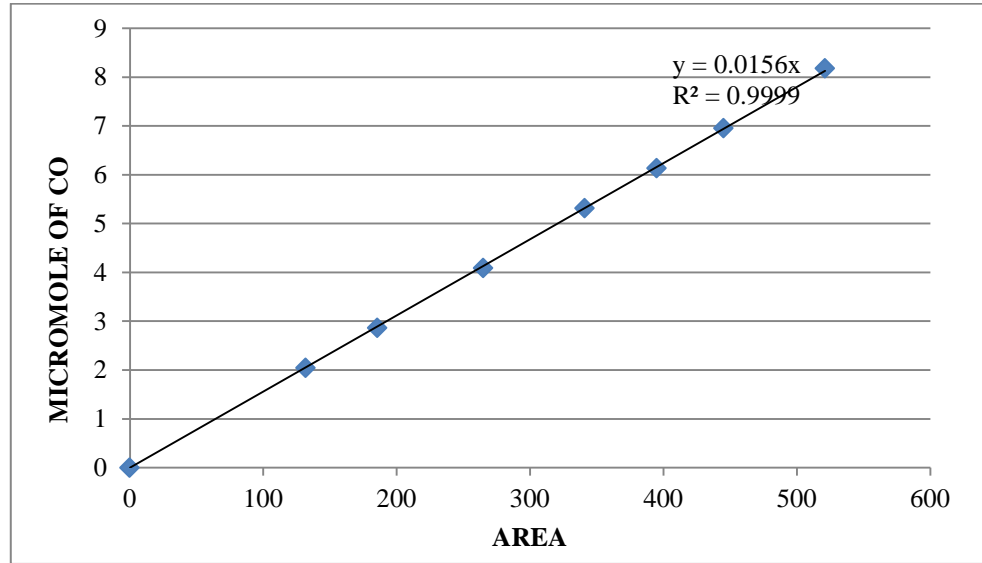


Figure A.3. Calibration curve of carbon monoxide

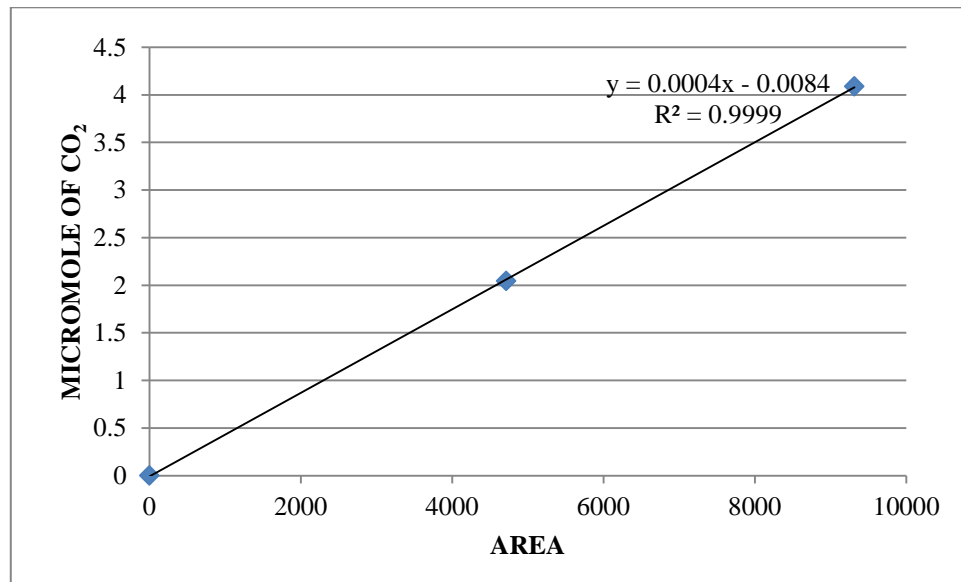


Figure A.4. Calibration curve of carbon dioxide

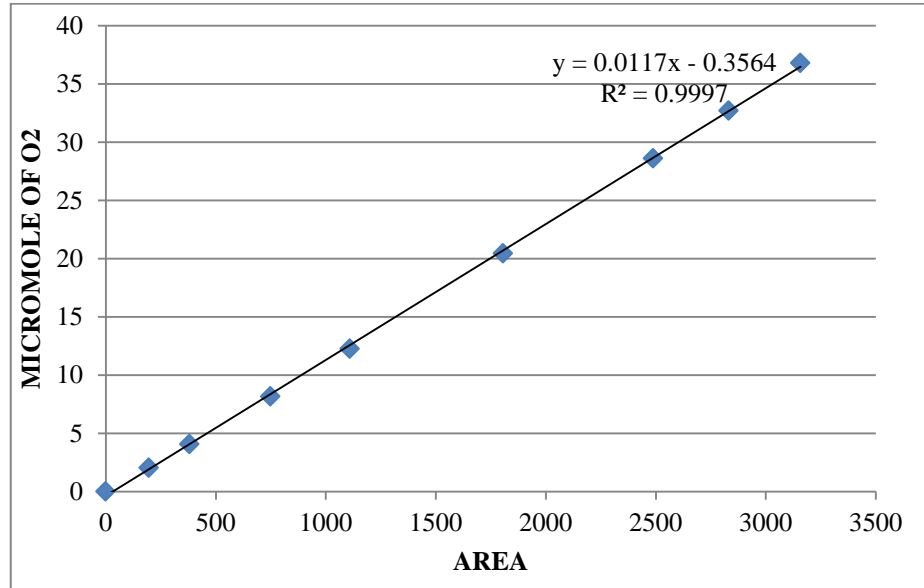


Figure A.5. Calibration curve of oxygen

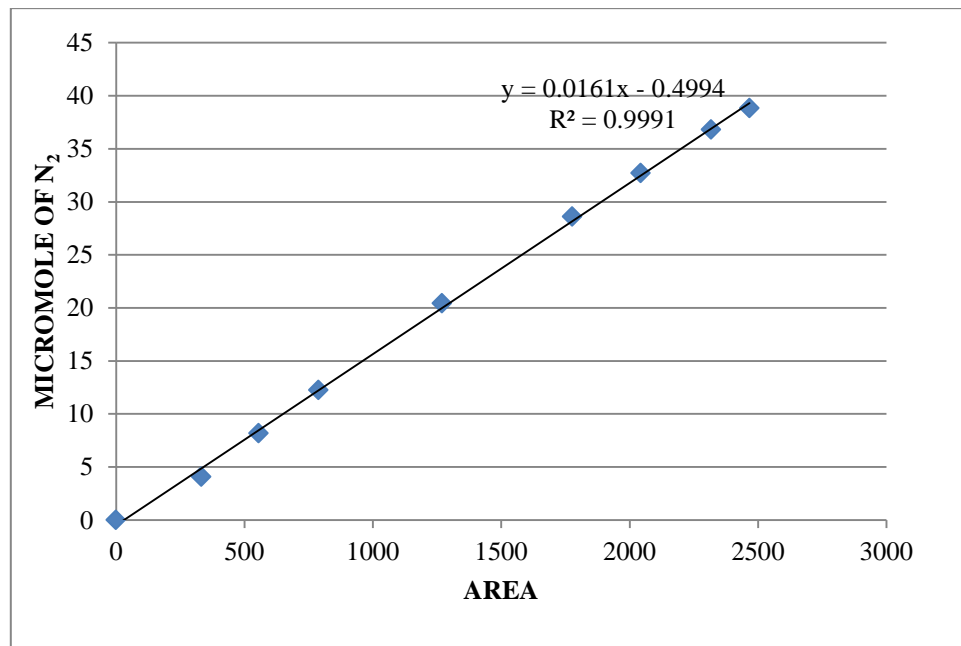


Figure A.6. Calibration curve of nitrogen

## APPENDIX B: CALIBRATION CURVES OF THE MASS FLOW CONTROLLERS

Calibration curves of the mass flow controllers used in the experiments are illustrated below.

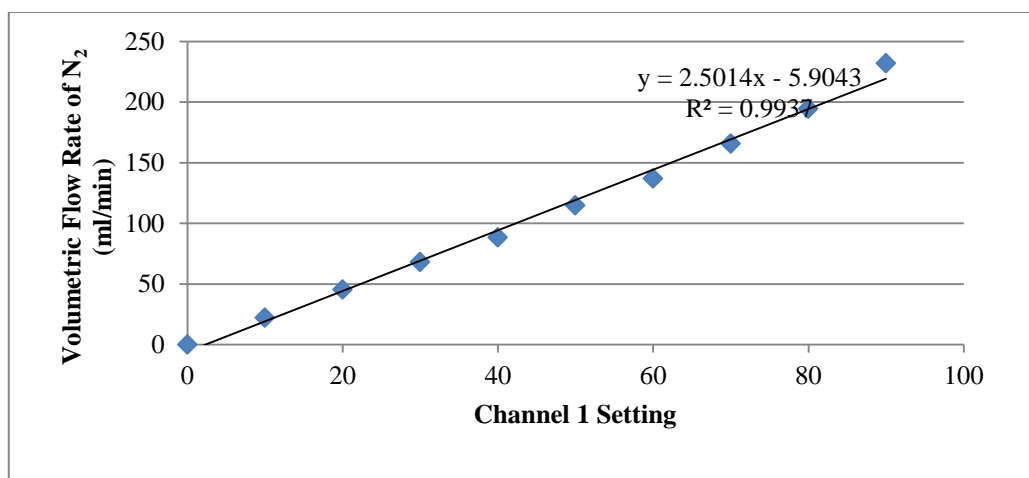


Figure B.1. Calibration curve of the nitrogen mass flow controller

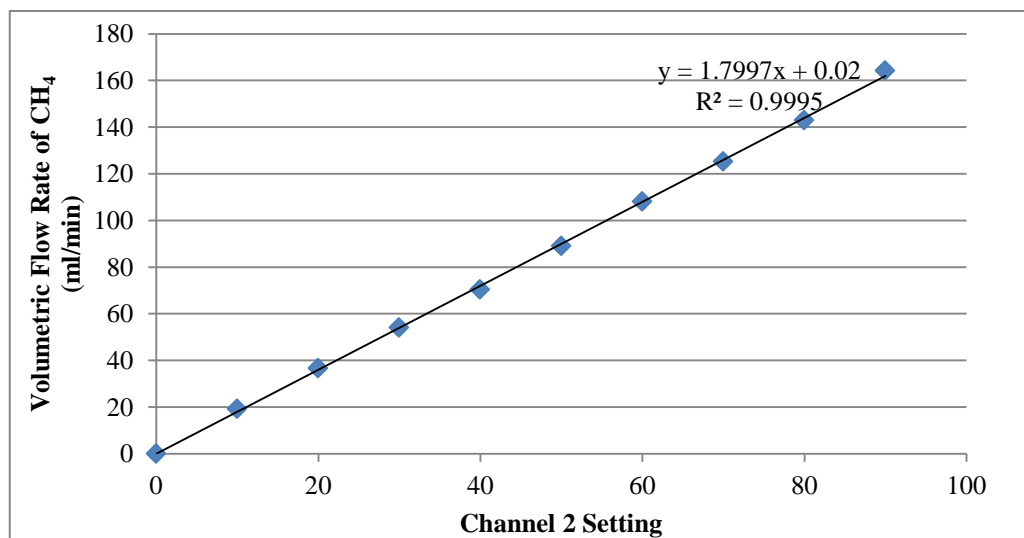


Figure B.2. Calibration curve of the methane mass flow controller

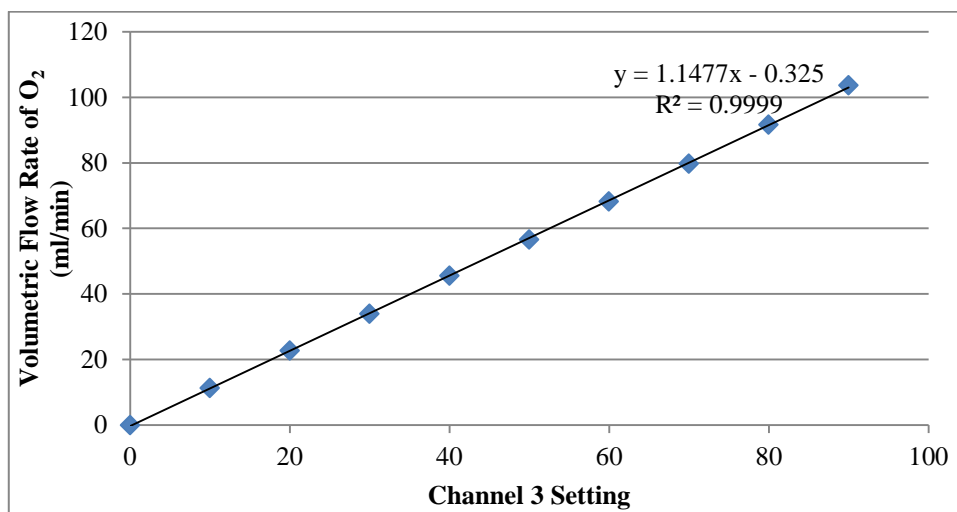


Figure B.3. Calibration curve of the oxygen mass flow controller

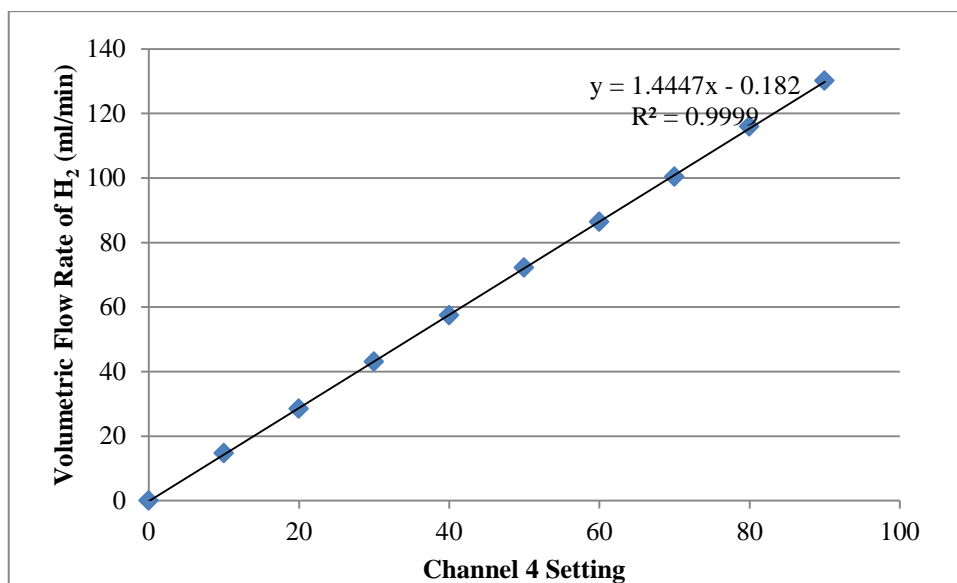


Figure B.4. Calibration curve of the hydrogen mass flow controller

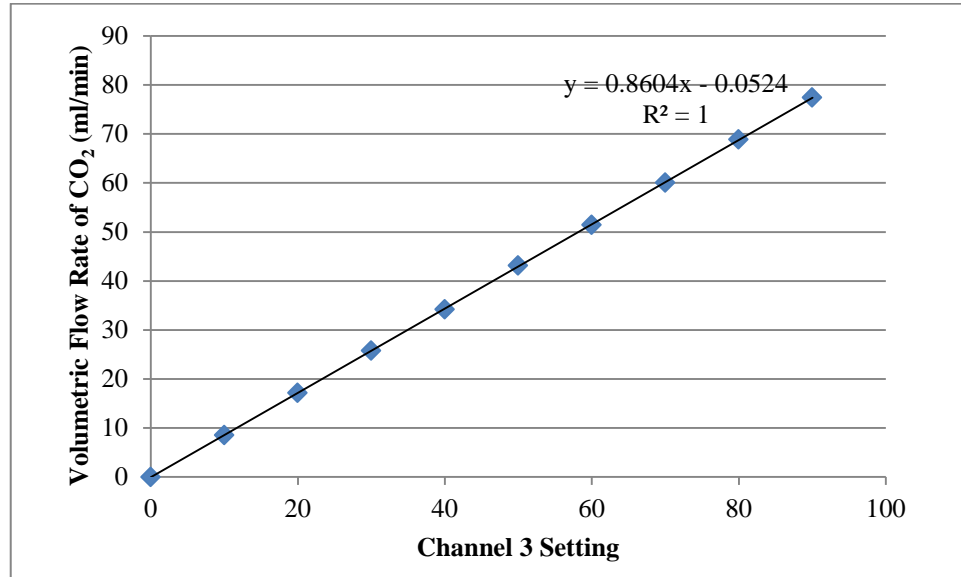


Figure B.5. Calibration curve of the carbon dioxide mass flow controller

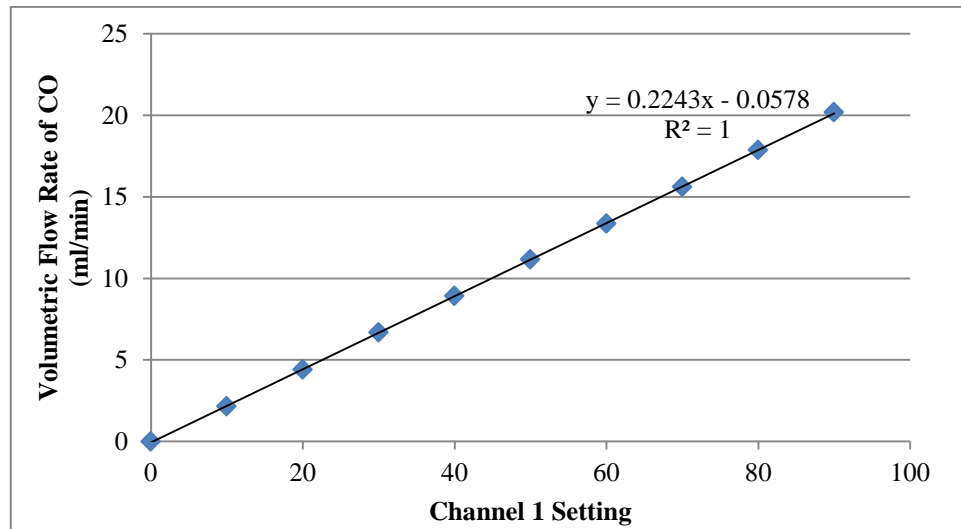


Figure B.6. Calibration curve of the carbon monoxide mass flow controller

## REFERENCES

- Ahmed, S. and M. Krumpelt, 2001, "Hydrogen from Hydrocarbon Fuels for Fuel Cells", *International Journal of Hydrogen Energy*, Vol. 26, pp. 291-301.
- Akın, A. N. and Z. İ. Önsan, 1997, "Kinetics of CO Hydrogenation over Coprecipitated Cobalt-Alumina", *Journal of Chemical Technology and Biotechnology*, Vol. 70, pp. 304-310.
- Avcı, A.K., D. L. Trimm and Z. İ. Önsan, 2002, "Quantitative Investigation of Catalytic Natural Gas Conversion for Hydrogen Fuel Cell Applications", *Chemical Engineering Journal*, Vol. 90, pp.77-87.
- Avcı, A. K., D. L. Trimm and Z. İ. Önsan, 2003, "On-board Hydrogen Generation for Fuel Cell Powered Vehicles: The Use of Methanol and Propane", *Topics in Catalysis*, Vol. 22, pp.359-367.
- Avcı, A.K., D.L. Trimm, A.E. Aksoylu and Z. İ. Önsan, 2004, "Hydrogen production by Steam reforming of *n*-butane over supported Ni and Pt-Ni catalysts", *Applied Catalysis A: General*, Vol. 258, pp. 235–240.
- Avcı, A.K., Ö. Tan, E. Maşalacı, Z. İ. Önsan, 2008, "Design of a methane processing system producing high-purity hydrogen", *International Journal of Hydrogen Energy*, Vol. 33, pp. 5516-5526.
- Barreto, L., A. Makihira, K. Riahi, 2003, "The Hydrogen Economy in the 21st Century: A Sustainable Development Scenario", *International Journal of Hydrogen Energy*, Vol. 28, pp. 267–284.

- Borowiecki, T., A. Goiebiowski, B. Stasinska, 1997, "Effects of small MoO<sub>3</sub> additions on the properties of nickel catalysts for the steam reforming of hydrocarbons", *Applied Catalysis A: General*, Vol.153, pp. 141-156.
- Borowiecki, T., G. Wojciech, D. Andrej, 2004, "Effects of small MoO<sub>3</sub> additions on the properties of nickel catalysts for the steam reforming of hydrocarbons: III. Reduction of Ni-Mo/Al<sub>2</sub>O<sub>3</sub> catalysts", *Applied Catalysis A: General*, Vol.270, pp. 27-36.
- Bradford, M.C.J., M.A. Vannice, 1999, "CO<sub>2</sub> Reforming of CH<sub>4</sub> over Supported Ru Catalysts", *Journal of Catalysis*, Vol. 183, pp-69-75.
- Brown, L.F., 2001, "A Comparative Study of Fuels for On-board Hydrogen Production for Fuel-Cell-Powered Automobiles", *International Journal of Hydrogen Energy*, Vol.26, pp. 381-397.
- Chen, CS, SJ Feng , S Ran , DC Zhu , W Liu and HJ Bouwmeester, 2003, " Conversion of Methane to Syngas by a Membrane-Based Oxidation–Reforming Process" *Angewandte Chemie International Edition*, Vol.115, pp.5354 –5356.
- Çağlayan, B.S, A.E. Aksoylu, 2011, "Water–gas shift activity of ceria supported Au–Re catalysts" *Catalysis Communications* Vol.12, pp.1206–1211.
- Dagle, R.A., A. Platon, D.R. Palo, A.K. Datye, J.M. Vohs, Y. Wang,2008, " PdZnAl catalysts for the reactions of water-gas-shift, methanol steam reforming, and reverse-water-gas-shift" *Applied Catalysis A: General*, Vol.342, pp.63-68.
- Giroux T., S. Hwang, Y. Liu, W. Ruettinger and L. Shore, 2005, "Monolithic structures as alternatives to particulate catalysts for the reforming of hydrocarbons for hydrogen generation, *Applied Catalysis B: Environmental*, Vol. 56 pp. 95-110.
- Gupta, R. B., 2009, *Hydrogen Fuel - Production, Transport, and Storage*, CRC Press, Florida.

- Güneş, H., 2009, “Study of Low Temperature Water Gas Shift Reaction on Promoted Au/Al<sub>2</sub>O<sub>3</sub> Catalysts” M. S. Thesis, Boğaziçi University.
- Halabi, M.H., M.H.J.M. de Croon, J. van der Schaaf, P.D Cobden, J. C Shouten, 2010, “ Low Temperature Catalytic Methane Steam Reforming Over Ceria-Zirconia Supported Rhodium” *Applied Catalysis A: General*, Vol: 386, pp. 68-79.
- Heck, R. M., S. Gulati and R. J. Farrauto, 2001, “The application of monoliths for gas phase catalytic reactions”, *Chemical Engineering Journal*, Vol. 82, pp.149-156.
- Holladay, J.D., J. Hu , D.L. King and Y. Wang, 2009, “An overview of hydrogen production Technologies” *Catalysis Today*, Vol.139 pp.244–260.
- Hordeski, M. F., 2009, *Hydrogen & Fuel Cells: Advances in Transportation and Power*, The Fairmont Press, Lilburn.
- Kusakabe, K., K.I. Sotowa, T. Eda ,Y. Iwamoto, 2004,” Methane steam reforming over Ce – ZrO<sub>2</sub>-supported noble metal catalysts at low temperature” *Fuel Processing Technology*, Vol. 86, pp. 319-326.
- Laosiripojana, N., S. Assabumrungant, 2005, “Methane Steam Reforming over Ni/Ce-ZrO<sub>2</sub> Calatyst: Influences of Ce-ZrO<sub>2</sub> Support on Reactivity, Resistance toward Carbon Formation, and Intrinsic Reaction Kinetics” *Applied Catalysis A: General*, Vol.290, pp. 210-211.
- Lee, H.D., D.V. Applegate, S. Ahmed, S.G. Calderone, T.L. Harvey, 2005, “Hydrogen from Natural Gas: Part I-Autothermal Reforming in an Integrated Fuel Processor”, *International Journal of Hydrogen Energy*, Vol. 30, pp. 829–842.

- Liu, S., G. Xiong, H. Dong, W. Yang, 2000, "Effect of carbon dioxide on the reaction performance of partial oxidation of methane over a LiLaNiO/ $\gamma$ -Al<sub>2</sub>O<sub>3</sub> catalyst" *Applied Catalysis A: General* Vol.202, pp. 141–146.
- Ma, L., 1995, Hydrogen Production from Steam Reforming of Light Hydrocarbons in an Autothermic System, Ph. D. Thesis, University of New South Wales.
- Matsukata, M., T. Matsushita, K. Ueyama, 1996, "A novel hydrogen/syngas production process: Catalytic activity and stability of Ni/SiO<sub>2</sub>" *Chemical Engineering Science*, Vol.51, pp.2769-2774.
- Nakayama, O., Na-oki Ikenaga, T.Miyake, E.Yagasaki and T.Suzuki, 2008 "Partial oxidation of CH<sub>4</sub> with air to produce pure hydrogen and syngas" *Catalysis Today* Vol.138 pp.141–146.
- Önsan, Z. İ, 2007, "Catalytic Processes for Clean Hydrogen Production from Hydrocarbons", *Turkish Journal of Chemistry*, Vol. 31, pp. 531-550.
- Öztürk, İ., 2009, "Construction and Testing of a Bench-Scale Reactor System for Autothermal Reforming of Methane", M. S. Thesis, Boğaziçi University.
- Paksoy, A.İ., 2010, "An Experimental Study on Design and Development of Efficient Catalysts for Dry Reforming of Methane (CDRM)", M. S. Thesis, Boğaziçi University.
- Pena, M.A., J.P. Gómez, J.L.G. Fierro, 1996, "New catalytic routes for syngas and hydrogen production" *Applied Catalysis A: General*, Vol.144, pp. 7-57.
- Profeti, L.P.R., E.A. Ticianelli, E.M. Assaf, 2008, "Co/Al<sub>2</sub>O<sub>3</sub> catalysts promoted with noble metals for production of hydrogen by methane steam reforming" *Fuel*, Vol.87, pp. 2076–2081.

- Requies, J., M.A. Cabrero, V.L. Barrio, M.B. Güemez, J.F. Cambra, P.L. Arias, F.J. Pe´rez-Alonso, M. Ojeda, M.A. Pena, J.L.G. Fierro, 2005, “Partial oxidation of methane to syngas over Ni/MgO and Ni/La<sub>2</sub>O<sub>3</sub> catalysts” *Applied Catalysis A: General*, Vol. 289, pp. 214–223.
- Rostrup-Nielsen, J.R., 1984, “Catalytic Steam Reforming”, in J.R. Anderson and M. Boudart (Eds.), *Catalysis, Science & Technology*, Vol. 5, pp. 1-117, Springer-Verlag, Berlin.
- Rostrup-Nielsen, J.R., 1994, “Catalysis and large-scale conversion of natural gas” *Catalysis Today*, Vol. 21, pp. 257-267.
- Rostrup-Nielsen, J.R., T. S. Christensen, Ib Dybkjaer, 1998, “Steam Reforming of Liquid Hydrocarbons”, *Studies in Surface Science and Catalysis*, Vol. 113, pp 81-95.
- Ruckenstein, E., H. Y. Wang, 1999, “Effect of Support on Partial Oxidation of Methane to Synthesis Gas over Supported Rhodium Catalysts”, *Journal of Catalysis*, Vol.187, pp-151-159.
- Salhi, N., A. Boulahouache , C. Petit , A. Kiennemann, C. Rabia, 2010, “ Steam reforming of methane to syngas over NiAl<sub>2</sub>O<sub>4</sub> spinel catalysts” *International Journal of Hydrogen Energy* XXX.
- Semelsberger, T. A., L. F. Brown, R. L. Borup, M.A. Inbody, 2004, “Equilibrium Products from Autothermal Processes for Generating Hydrogen- Rich Fuel- Cell Feeds”, *Internatioanl Journal of Hydrogen Energy*, Vol 29, pp. 1047-1064.
- Sperle, T., D. Chen, R. Lødeng, A. Holmen, 2005, “Pre-reforming of natural gas on a Ni catalyst: Criteria for carbon free operation”, *Applied Catalysis A: General*, Vol.282, pp. 195-204

- Steynberg, A.P and M.E. Dry, 2004 “Fischer-Tropsch Technology” *Elsevier Science & Technology Books*.
- Souza, M. M. V. M, O.R.M. Neto, M. Schmal , 2006, “ Synthesis Gas Production from Natural Gas on Supported Pt Catalysts” *Journal of Natural Gas Chemistry*, Vol.15, pp. 21-27.
- Şen, Ö., 2008, *Constructing and Testing of a Low-Temperature Water-Gas Shift Reaction System*, M. S. Thesis, Boğaziçi University, Istanbul.
- Trimm, D. L. And Z. İ. Önsan, 2001, “Onboard Fuel Conversion for Hydrogen-Fuel-Cell-Driven Vehicles”, *Catalysis Reviews: Science and Engineering*, Vol. 43, pp. 31-84.
- Tsang, S. C., J.B. Claridge, M.L.H. Green, 1995,“ Recent advances in the conversion of methane to synthesis gas” *Catalysis Today*, Vol.23, pp. 3-15.
- Wang, X., R. J. Gorte, 2002, “A study of steam reforming of hydrocarbon fuels on Pd/ceria” *Applied Catalysis A: General*, Vol.224, pp.209–218.
- Wu, P., X. Li, S. Ji, B. Lang, F. Habimana, C. Li, 2009, “ Steam reforming of methane to hydrogen over Ni-based monolith catalysts” *Catalysis Today*, Vol. 146, pp. 82-86.
- Yan,Q.G., W.Z. Weng, H.L. Wan, H. Toghiani, R.K. Toghiani, C.U. Pittman, Jr., 2003, “Activation of methane to syngas over a Ni/TiO<sub>2</sub> catalyst” *Applied Catalysis A: General*, Vol. 239, pp. 43–58.
- Zhang, Z.L., V. A. Tsipouriari, A. M. Efstathiou, and X. E. Verykios, 1996, “Reforming of Methane with Carbon Dioxide to Synthesis Gas over Supported Rhodium Catalysts I. Effects of Support and Metal Crystallite Size on Reaction Activity and Deactivation Characteristics” *Journal of Catalysis*, Vol.158, pp. 51-63.